Calibration and Evaluation of Building Energy Models to Assess and Mitigate Canadian Building Overheating Risks in Current and Future Climates

Kathryn Chung Tze Cheong

A Thesis
in
the Department
of
Building, Civil and Environmental Engineering

Presented in Partial Fulfilment of the Requirements
for the Degree of
Master of Applied Science (Building Engineering) at
Concordia University
Montreal, Quebec, Canada

August 2023

CONCORDIA UNIVERSITY
SCHOOL OF GRADUATE STUDIES

This is to certify that the thesis prepared

By: Kathryn Chung Tze Cheong

Entitled: Calibration and Evaluation of Building Energy Models to Assess and Mitigate Canadian Building Overheating Risks in Current and Future Climates

and submitted in partial fulfillment of the requirements for the degree of

Master of Applied Science (Building Engineering)

Complies with the regulations of the University and meets the accepted standards with respect to originality and quality.

Signed by the final Examining Committee:

_____ Chair

Dr. Bruno Lee

_____ Examiner

Dr. Caroline Hachem-Vermette

_____ Supervisor

Dr. Liangzhu (Leon) Wang

_____ Supervisor

Dr. Hua Ge

Approved by: _____

Chair of Department or Graduate Program Director

August 2023 _____

Dean of Faculty

Abstract

Calibration and Evaluation of Building Energy Models to Assess and Mitigate Canadian Building Overheating Risks in Current and Future Climates

Kathryn Chung Tze Cheong

Climate change continues to impact weather conditions globally, requiring cities to adapt to new environments. In Canada, indoor summer overheating in buildings is problematic due to their primary design for cold winters, making them susceptible to extreme heatwave events. This research focuses on calibrating building models and employing model calibration methodologies to evaluate and address overheating risks in various building types across Canada using current and future weather data. The study's objectives are to accurately assess summertime overheating risks in selected buildings in Montreal, Quebec, and evaluate effective mitigation strategies. Bayesian calibration and multi-objective genetic algorithms are used as calibration methods, with the latter showing superiority in producing highly accurate calibrated models based on five performance criteria. By incorporating field measurements and novel methodologies, the research ensures precise assessment and mitigation of summertime overheating risks. After calibrating several buildings, including schools, a hospital, and a residential building, which demonstrates the reliability and repeatability of the calibration process, the assessment of overheating is conducted on calibrated models to determine the number of overheating hours during the summer. In conclusion, this thesis demonstrates the repeatability of the calibration methods on a variety of existing Canadian buildings and the effective use of passive cooling techniques, such as external shading, night cooling, and high albedo surfaces, that are implemented in the building models, to mitigate overheating based on current and future weather data.

Acknowledgments

I would like to express my heartfelt gratitude to all those who have supported and contributed to the completion of this research project.

First, I extend my appreciation to my supervisors, Dr. Liangzhu (Leon) Wang and Dr. Hua Ge, whose invaluable guidance, expertise, and encouragement have bene instrumental throughout this journey. Their mentorship and support have played a pivotal role in shaping the direction and quality of this research.

I am also grateful to all my colleagues who were part of the NSERC Summertime Overheating Project, who provided valuable insights, feedback, and generous eagerness to share resources and expertise during my time at Concordia. I would like to thank Daniel Baril and Zihan Xie for their contributions in preparing and collecting field measurements from the buildings studied in this thesis; and Dr. Danlin Hou, Dr. Fuad Baba, Dr. Lili Ji, and Dr. Chang Shu for their extensive involvement in sharing their knowledge and understanding in calibration methods, development and applications to this project. The final work presented in this thesis could not have been completed without their help.

I would like to acknowledge the support from Hydro-Quebec's Graduate Studies Scholarship and NSERC for providing the necessary financial assistance, which made this research possible.

Lastly, I want to extend my appreciation to my friends and family who have been there for me throughout this process for their unwavering support and encouragement, helping me push through all my highs and lows.

Table of Contents

List of Figures

List of Tables

Nomenclature

ACH	Air changes per hour
BC	Bayesian calibration
CV(RMSE)	Coefficient of variation of the root mean squared error
EPD	Equipment power density
EPW	Weather file
GA	Genetic algorithm
LPD	Lighting power density
MLR	Multiple linear regression
MOGA	Multi-objective genetic algorithm
NMBE	Normalized mean bias error
NVA	Natural ventilation ACH
NVS	Natural ventilation setpoint
OCC	Number of occupants
RCP	Representative concentration pathways
RF	Random forests
RSWY	Reference summer weather year
RUV	Roof insulation U-value
SA	Sensitivity analysis
SHGC	Solar heat gain coefficient for window glazing
SR	Solar reflectance of interior diffusing shade roll
SVI	Sensitivity value index
TMY	Typical meteorological year
WALU	Wall insulation U-value
WINU	Window insulation U-value
WWR	Window-to-wall ratio

1. Introduction

1.1. Background

Climate change is being experienced in many different ways around the world. Earth's global average surface temperature has increased steadily by 0.7°C since 1900 (Chidiac et al., 2022). As a global average, different areas of the planet are experiencing the effects of this temperature increase in a variety of extreme weather events, such as heatwaves, floods, earthquakes, forest fires, hurricanes, tsunamis, etc. In Canada, the country's average annual temperature has risen by 1.7°C since 1948, which is more than twice the global average temperature rise, resulting in climate change having an even greater impact in this region (Zhang et al., 2019). While increasing temperatures may not seem to be very detrimental for a country that is known for its colder climate, this temperature increase is causing summertime overheating in many ill-equipped buildings and is becoming a health issue for those who are affected (Baba et al., 2022a). For example, Quebec experienced a severe heatwave in 2018 that resulted in at least 66 deaths (Oetomo et al., 2022). And so, this increase in surface temperature is becoming problematic, especially to older adults, persons with disabilities, persons with chronic conditions and children who are more vulnerable during extreme heat days due to their impaired ability to regulate their body temperature (Oetomo et al., 2022).

In addition to increasing surface temperatures having an influence on climate change, greenhouse gas emissions related to energy use, along with urbanization and changes in land use are one of the main causes of climate change (Chidiac et al., 2022). Buildings in particular, are responsible for approximately 32% of global final energy use, 17% of direct carbon dioxide emissions and 33% of indirect emissions (Skillington et al., 2022). In this respect, efforts have been made to reduce energy use and related greenhouse gas emissions in buildings to reduce climate change effects due to buildings by making them more energy efficient. A solution to improving buildings' energy use often leads to increasing building envelope insulation to reduce heating costs, especially in cold climates. However, this is proving to be challenging during the summer for buildings that are unable to release excess heat and/or end up requiring excessive use of mechanical cooling. And this overheating is extremely harmful for older buildings that are not equipped with mechanical ventilation, as mechanical ventilation and/or air conditioning was not historically required in all building types.

Between the rising global surface temperature and the greenhouse gas emissions causing climate change and buildings seeking highly energy-efficient building envelopes in colder climates, overheating is becoming a significant problem in Canada (Berardi et al., 2020). Previous studies have already concluded that the risk of overheating will increase in the future due to climate change and the trend toward high energy-efficient envelopes (Baba et al., 2022a). With an increasing emphasis on the quality of the built environment and a growing focus on building energy efficiency, building simulation has become an indispensable tool for design, validation, and analysis (Mahmoud et al., 2022). Subsequently, this technology can and will be used to assess overheating risks in both existing and new construction.

1.2. Research objectives

This research examines the calibration of building models to assess and mitigate the risks of overheating in various building types in Canada, as a part of the project funded by the National Research Council Canada (NRC) and the Natural Sciences and Engineering Research Council (NSERC) on the "Assessment and Mitigation of Summertime Overheating Conditions in Vulnerable Buildings of Urban Agglomerations". The work shown in this thesis follows the selection of buildings, field monitoring and data collection, whole building simulations and urban scale simulations, in order to come to this part of the project that involves the calibration of buildings and the assessment and mitigation of overheating risks in buildings.

The impact of climate change on indoor summer overheating in Canadian buildings is expected to be more significant than in other climates, given that Canadian buildings have been primarily designed to withstand cold and long winters, not hot summers, especially in buildings that house vulnerable people, such as the elderly, children or residents with pre-existing health conditions (Baba et al., 2023). With the recent change in Canada's climate, existing Canadian buildings have not all been adapted to withstand higher summertime temperatures and research in assessing the overheating risks and retrofit solutions is limited. Global weather statistics show that the average global temperature on Earth has been rising faster over time, having increased by about 0.8°C since 1880, with two-thirds of this warming having occurred since 1975 (Lessen et al. 2019). And so, it is unsurprising that most school buildings that were built before 1970, which represent 64% of all schools in Quebec (Gouvernement du Québec, 2021), and 58% of residential buildings in Canada (Baba et al., 2022a) are not equipped with air conditioning units and are at risk for overheating. Additionally, in a study looking at indoor temperatures during the 2018 heatwave in Quebec, Canada, non-air-conditioned homes experienced a greater than 1°C difference in temperature between heatwave and non-heatwave days (Oetemo et al., 2022).

To resolve problems of overheating, the risk of summertime overheating is assessed and mitigation strategies are evaluated in this thesis using calibrated building models. Simulation programs are invaluable tools that aid engineers in expediting the design process, mitigating critical flaws, and enhancing overall efficiency (Mahmoud et al., 2022). A variety of simulation tools will enable modelling of existing buildings and running of simulations over measured and future climate data files to allow further investigation into building overheating issues. However, the gap between modelled and actual energy performance remains one of the most discussed concerns in the building design community (Moradi et al., 2023). And so, to bridge the gap between modelled and actual building data and performance in the context of summertime overheating, building model simulations and model calibrations using field measurements will be performed using recently developed building model calibration methodologies to accurately assess the risk of overheating in the selected buildings located in Montreal, Quebec, Canada.

Lastly, model calibration plays an important role in reducing the discrepancy between the simulation value and the measured data (Li et al. 2018). A calibrated thermal performance model will better guide building retrofits and optimized operations to address overheating (Li et al., 2018). Two calibration methodologies will be evaluated to select one methodology that is more suited to accurately calibrate different building types in Quebec, Canada. One methodology was developed by Hou et al. using Bayes' Theorem to auto-calibrate building models while minimizing

computing time and maximizing model accuracy (Hou et al., 2021a). Another robust methodology was developed by Baba et al. to create a building model with high accuracy prediction of indoor air temperature compared to measured data (Baba et al., 2022b). Using calibrated models with measured indoor data and running simulations with measured and future climate data will ensure a highly accurate assessment and mitigation of summertime overheating risks.

1.3. Outline of the Thesis

This thesis is composed of the following chapters:

Chapter 1 – Introduction

Chapter 2 – Literature review: This chapter includes four parts: model calibration types and methods; sensitivity analysis method used to determine important unknown building parameters; use of current and future weather data for overheating risk assessment; and thermal comfort criteria for the evaluation of occupant comfort in indoor environments.

Chapter 3 – Calibration methodology: This chapter provides details on the application of two calibration methods and the performance criteria used to evaluate the accuracy and precision of these methods.

Chapter 4 – Comparison of calibration methods: This chapter presents the calibration results of one school's building models using two different calibration methods.

Chapter 5 – Application of the MOGA methods on schools, hospitals and residential buildings: This chapter provides a summary of the calibration results and performance criteria following the calibration of different types of buildings using MOGA.

Chapter 6 – Assessment and mitigation of summertime overheating: This chapter provides a summary of the summertime overheating risks and proposed solutions to mitigate these risks on schools, hospitals and residential buildings in current and future climates.

Chapter 7 – Conclusions and discussions: This chapter summarizes the key findings and main contributions of this thesis.

2. Literature Review

2.1 Model Calibration

Building energy models can be used during the initial design phases to optimize energy efficiency, as well as with existing buildings to evaluate their current energy performance. Although the building energy simulation software is quite mature, large discrepancies exist between building energy simulation and measured data (Li et al., 2018). This can be caused by a number of factors including, but not limited to occupancy behavior, malfunctioning or unexpected functioning of building services, changes in building use, extreme weather events, etc. In an attempt to take into account these variable factors, model calibration is necessary to provide a more accurate picture of the building's situation, by fine-tuning input parameters of the simulation model to minimize discrepancies with the existing building (Lim and Zhai, 2018). To do this, there are two methods of building model calibration that can be classified into two broad categories of manual calibration and automated calibration (Zhu et al., 2020).

2.1.1. Types of Calibration

Manual calibration refers to the manual adjustment of the input parameters of the model by comparing the discrepancy between the output of the thermal performance model and the actual measured data according to the user's professional knowledge (Li et al., 2018). This method can be a lengthy process and requires a person who is an expert in the field. Automatic calibration takes building thermal performance model calibration as a mathematical optimization process, and automatically adjusts the model input parameters according to certain constraints to minimize the difference between simulated values and actual values (Li et al., 2018). This method should allow users with limited knowledge to produce highly accurate models. Historically, automatic calibration methods have been known to require a high amount of computing time, causing it to still be a lengthy and costly process in some cases. However, with the advancement of computers, automated calibration can now match the simulation results to the measured data with an acceptable error and considerably faster than manual calibration (Derakhti et al., 2022). There exists a few automated approaches in development that include Bayesian analysis, pattern matching, and multi-objective optimization (Zhu et al., 2020). More recent research has focused on these automated approaches since it can increase the accuracy of calibrated models and improve the consistency of the calibration process.

2.1.2. Bayesian Calibration

This type of automated calibration uses Bayesian Inference which is the process of fitting a probability model to a data set and summarizing the results by using a probability distribution on the parameters of the model and unobserved quantities (Hou et al., 2021b). Even though Bayesian Inference Statistics can be derived from over two hundred years ago, it has only begun to experience significant advancements in recent years with the development of computer techniques and advanced statistical theory (Hou et al., 2021a). Still, it is a time-consuming process that has been refined by using simplified energy models, namely meta-models to represent the original building energy model, to reduce the calculation time of Bayesian Calibration (Lim and Zhai, 2018). It has been previously confirmed that multi-linear regression models could generate

reasonable calibration results that significantly reduced computing and therefore was selected for the meta-model (Lim and Zhai, 2018). Furthermore, Monte-Carlo-Markov-Chain method is employed to further reduce the computational burden as discussed in a methodology developed by Hou et al. (Hou et al., 2021b).

2.1.3. Multi-Objective Genetic Algorithm

Genetic algorithm is one of many optimization techniques for automated calibration from the evolutionary algorithm family (Derakhti et al., 2022). This algorithm determines a potential solution to a specific problem by evolving a population of individuals (Derakhti et al., 2022). Using this technique, a study by Baba et al. developed a robust methodology to create a building model with high accuracy prediction of indoor air temperatures compared to measured data (Baba et al., 2023). This methodology allows the simultaneous calibration of multiple rooms in the same building using global variance-based sensitivity analysis to reduce the number of unknown building parameters by calibrating only the parameters with significant impact on indoor temperature (Baba et al., 2023). In this thesis, jePlus + EA is used to calibrate several buildings in Montreal, Quebec, Canada. It utilizes a multi-objective optimization algorithm for building optimizations as explored in a study evaluating energy-saving measures and operation parameters for a newly retrofitted building by Gao et al. (Gao et al. 2023).

2.2. Sensitivity Analysis

Both above-mentioned automated calibration methods utilize sensitivity analysis, to reduce the number of parameters to calibrate and further reduce computing time and extensive computing loads. Sensitivity analysis can reduce the number of parameters to calibrate and improve the calibration efficiency (Li et al., 2018). The less significant parameters can be left out of calibration to enhance the efficiency of the calibration process because very little variance of the final output can be observed by tuning these particular parameters as determined by sensitivity analysis (Qiu et al., 2018). This is an important step in the calibration process that has two types of analyses: local sensitivity and global sensitivity. Local sensitivity is the simplest method that can be used to estimate the influence of the inputs on the output by changing the value of each variable separately (Derakhti et al., 2022). This type of analysis observes one parameter at a time to optimize each factor individually. However, with a system as complex as a building where variables are most often interacting with each other, optimizing one parameter at a time may not guarantee a holistic optimal solution. Therefore, global sensitivity methods are used by Bayesian and multi-objective genetic algorithm calibration methods to quantify the sensitivity of a parameter of the model by varying all design parameters simultaneously (Derakhti et al., 2022).

2.3. Current and Future Weather Data

To evaluate the overheating risks in the present and for the future, both present and future weather data must be used. This is especially important in evaluating mitigation strategies to best recommend solutions that have a lasting effect on the building now and in the coming years. When it comes to new buildings, design decisions and climate change, mitigation strategies are going to affect the buildings' performance and their ability to withstand short and long-term climate events for the next 50 to 120 years, being the typical service life of a building (Kim et al., 2023). And

while in this study, the focus was evaluating existing buildings, major renovations that involve introducing building features to mitigate overheating risks in future climates could extend the service life of these existing buildings by at least 50 years (Baba et al., 2023).

In this section, typical weather data and future climate data are described to rationalize the use of future climate data for overheating risk assessment. First, typical weather data files include information based on recent historic weather trends to predict future data (Baba et al., 2022a). These data files are suitable for assessing overall energy consumption in buildings. However, overheating assessment needs to take extreme weather events into account and requires inclusion of extreme climactic data in the weather file that typical weather data files do not have (Baba et al., 2023). Second, future climate data was developed by Baba et al. to create a Reference Summer Weather Year (RSWY), which includes multi-year weather data to represent the extreme weather years that focuses on specific years in historical, mid-, and long-term periods which experience the most intense, severe and/or long heatwaves (Baba et al., 2023). Heatwave periods are defined by Environment Canada as periods of at least three consecutive days during which temperatures reach or exceed 30°C during the day (Li et al., 2018; Ville de Montreal, 2017). RSWY files were generated using IPCC's reports with varying levels of expected severity of global warming due to climate change that is quantified by RCP values to project greenhouse gas emission levels (Baba et al., 2022b). With these reference summer weather files as opposed to historical typical weather files, extreme weather events that include increased frequency, severity and duration of heatwaves can be considered. And, so the use of future weather files, as opposed to typical weather data that relies on historical climate data, attempts to provide a clearer, more accurate picture of the overheating risks of each building.

2.4. Thermal Comfort Criteria

Finally, to assess overheating risk which constitutes the core of this study, thermal comfort criteria systems were selected to evaluate the acceptability of indoor thermal comfort in the buildings in question. And in conjunction with the previous section, the periods of time that are evaluated for overheating risk are during expected heatwave periods, to assess the building during the most extreme weather conditions. And simulating these extreme scenarios is made possible by the use of future extreme summer weather year data files. Subsequently, the definition of overheating in this thesis to assess the risk during current and future climates is defined by the following criteria, as calculated by the adaptive ASHRAE 55 method and CIBSE TM52. These criteria use the equations defined below to determine the an acceptable amount of hours in a given time period that may surpass the occupants level of thermal comfort. ASHRAE 55's 80% acceptability limit was used to assess the overheating for the residential and hospital buildings over the entire year, while BB101, which is based off CIBSE TM52 was used for school buildings over the months of May to September, from 9:00 to 16:00. The use of these thermal comfort criteria systems follows common use in evaluation of overheating and the study by Baba et al. exploring possible causes of overheating risks due to increasing energy-efficiency in buildings (Baba et al., 2022a).

2.4.1. ASHRAE 55's 80% Acceptability Limit/BC Energy Step Code

The most common standards developed to deal with adaptive thermal comfort are ASHRAE 55 and EN1521 (Baba et al., 2022a). Even though they have similar thresholds, ASHRAE 55 is still

chosen because it is more commonly used in North America (Baba et al., 2022a). This standard evaluates thermal comfort in naturally ventilated zones based on operative temperature, and overheating is considered to occur when this temperature exceeds the upper threshold temperature (Baba et al., 2023), which is described in the equations 2-1 and 2-3 below. These equations calculate the duration of overheating hours, time for which the indoor operative temperature (calculated by equation 2-3) of a room exceeds the acceptability limit of 80% that considers humidity, clothing discomfort, metabolic rate and air speed (Baba et al., 2023).

Upper 80% acceptability limit: $T_{up} = 0.31 \times T_{pma(out)} + 21.3$ Eq. (2-1)

Lower 80% acceptability limit: $T_{lower} = 0.31 \times T_{pma(out)} + 14.3$ Eq. (2-2)

$T_{op} = \frac{(T_r + T_{mrt})}{2}$ Eq. (2-3)

Using these criteria, the BC Energy Step Code (BCESC) and the City of Vancouver Zero Emissions Building Plan determined that overheating hours must not exceed 200 hours for regular occupants and 40 hours for vulnerable people (elderly, children and/or ill) during the summertime (which includes the months of May to September) to stay within the acceptable limit when studying overheating in buildings (Baba et al., 2022b).

2.4.2. CIBSE TM52/59 and BB101 for Schools

Another commonly used thermal comfort criteria is established by CIBSE, which requires two of three criteria to be fulfilled according to TM52, such as Hours of Exceedance, Daily Weighted Exceedance and Upper Limit Temperature (Escandón et al., 2022). Using these criteria, in the UK, Building Bulletin 101 (BB101) provides a design framework for school buildings, as described below where occupancy is expected from 9:00 to 16:00, May to September:

1. Hours of Exceedance (H_e) must less than or equal to 40 hours.
2. Daily Weighted Exceedance (W_e) must be less than or equal to 6 hours.
3. Upper Limit Temperature (T_{upp}) represents the maximum indoor operative temperature, with the condition that $\Delta T = T_{upp} - T_{max}$ must be less than or equal to 4 K (Escandón et al., 2022). Eq. (2-4)

These criteria are built into DesignBuilder to provide an assessment for overheating hours during building simulations and is consequently used to determine which mitigation strategies can offset these overheating hours.

3. Methodology

As mentioned earlier, this research is a part of the NSERC project "Assessment and Mitigation of Summertime Overheating Conditions in Vulnerable Buildings of Urban Agglomerations". In the earlier stages of this project, numerous buildings in Montreal were selected and evaluated in order to select a final roster of buidings to be studied for this project. Once selected, these buildings were equipped with indoor temperature sensors and humidity sensors, often in the rooms that were known to experience the most severe overheating according to building surveys with building managers and/or building occupants. Selected buildings were also equipped with local weather stations that were installed on their roofs. These weather stations collected various weather data including temperature, humidity, wind spped, etc. All measurement devices collected data in 10-min intervals. This raw data was then converted to hourly data in Excel to complete the calibration process. And while the weather station data could be accessed wirelessly, the indoor sensors had stored data that needed to be accessed in person every few months. Following the data collection of building information and field monitoring data, the calibration portion of the project began with the methodologies presented in this thesis.

Two methods were used in this thesis to calibrate building models, which include four school buildings, one hospital building and one residential building. The first method used and introduced here was Bayesian Calibration (BC) and the second method is Multi-Objective Genetic Algorithm (MOGA). The preparation of field measurements, building model and sensitivity analysis can be used for both methods. It is at the calibration step where the calculation process is different. This means that both processes go through the following steps: preparing data, model geometry, sensitivity analysis, calibration, and validation. This chapter first covers a section to describe the calibration process for each method and is then followed by the description of common steps that both methods share in more detail, including the tools used, building parameter ranges, sensitivity analysis, evaluation criteria and calibration and validation periods.

3.1. Bayesian Calibration

Hou et al. developed this methodology by extensively researching Bayesian Inference and its application to the calibration of building energy models (Hou et al., 2021c). It has 6 main steps that are explained below and were developed using R-code with RStudio and EnergyPlus.

Step 1: Measurements and Preparation
In the first step of this process, data must be collected and prepared to be used in conjunction with the prepared R-code. Outdoor weather data, specifically the dry-bulb temperature that is collected by the respective buildings' weather station, and the indoor air temperature of each of the measured rooms must be collected. This data is recorded in 10-minute intervals, so it must be converted in Excel to be used as hourly data. This process takes the average of the measured values within each hour to produce the estimated hourly data. Approximately 3 weeks of data for the calibration step and the following 3 weeks of data for the validation period are the ideal time periods to work with. Anything under two weeks would be too short of a time frame, while over 4 weeks could possibly incur drastic changes in occupational behaviors as seen in the literature (Baba, 2022).

Step 2: Building Energy Modelling
A building energy model of the building is required to perform the parametric simulation, using the building geometry, separate thermal zones for each room in the building and the building orientation. Parametric simulation is performed using set ranges and distributions commonly used in practice for unknown model building parameters. This creates a dataset that will be used in later steps.

Step 3: Sensitivity Analysis
Using the dataset generated in the previous step, a sensitivity analysis is performed. This step reveals which building parameters have the most impact on the temperature fluctuations in the building. The sensitivity analysis code calculates the t-value, SRC value and random forest value of each building parameter, which can then be used to calculate each parameter's SVI. The parameters with the highest SVI have the greatest effects on the indoor building temperature, therefore these are the parameters that need to be prioritized while calibrating the models.

Step 4: Meta-Model Development
With the same dataset, the original building model can be compressed, and a separate meta-model is created for each of the monitored rooms. Compressing the building model will decrease the calibration processing time.

Step 5: Bayesian Inference Calibration
Bayesian Inference is performed using Markov Chain Monte Carlo (MCMC), which will output calibrated values for the unknown building parameters that have high importance rank as calculated by the sensitivity analysis. The calibrated values will help align the simulation results to the actual measurements.

Step 6: Validation and Analysis
Once the calibrated indoor measurements are compared to the monitored results over the calibration period, the calibrated model is then used to produce indoor measurements over the validation period to be compared again to the monitored results. This step is different from the previous one because it is using the calibrated values from the calibration period to predict the values from the validation period that follows the calibration period. These results can then be further analyzed.

3.2. Multi-Objective Genetic Algorithm

Building calibration, as well as assessment and mitigation of overheating risks were performed using the MOGA method. Following the selection of buildings to collect thermal data for overheating risk assessment, building information and data needs to be collected. This includes conducting preliminary research on the building materials, type, use/function, location, year of construction, building plans, etc. With this data, an uncalibrated building energy model can be created in DesignBuilder using building information, site conditions, building geometry, orientation, location and materials. Then, field measurements of the building's indoor thermal conditions and exterior weather conditions must be gathered. Using collected field data and the uncalibrated model, a calibrated building energy model can be created by calibrating and validating the unknown parameters. Unknown parameters are defined in this thesis as the

parameters to be calibrated that have the greatest impact on the building model. The precision of the final calibrated parameters is evaluated against a set of performance criteria. Once the unknown parameters meet the performance criteria targets, the resulting building energy model is a highly precise calibrated building energy model that is ready to be used for the assessment of overheating. While the calibration process is performed over a 3-week period during the summer months, the overheating assessment is conducted over the entirety of one year to calculate the number of hours that the building surpasses a specified temperature in a year according to ASHRAE 90 standards for hospitals and residential buildings or CIBSE TM52 for school buildings. Once this step is completed, several mitigation techniques are then applied to the building to reduce the number of overheating hours to an acceptable level. These final two steps are subsequently replicated during future extreme weather years to identify which mitigation techniques, or their combinations, will yield a sustained effect on the building.

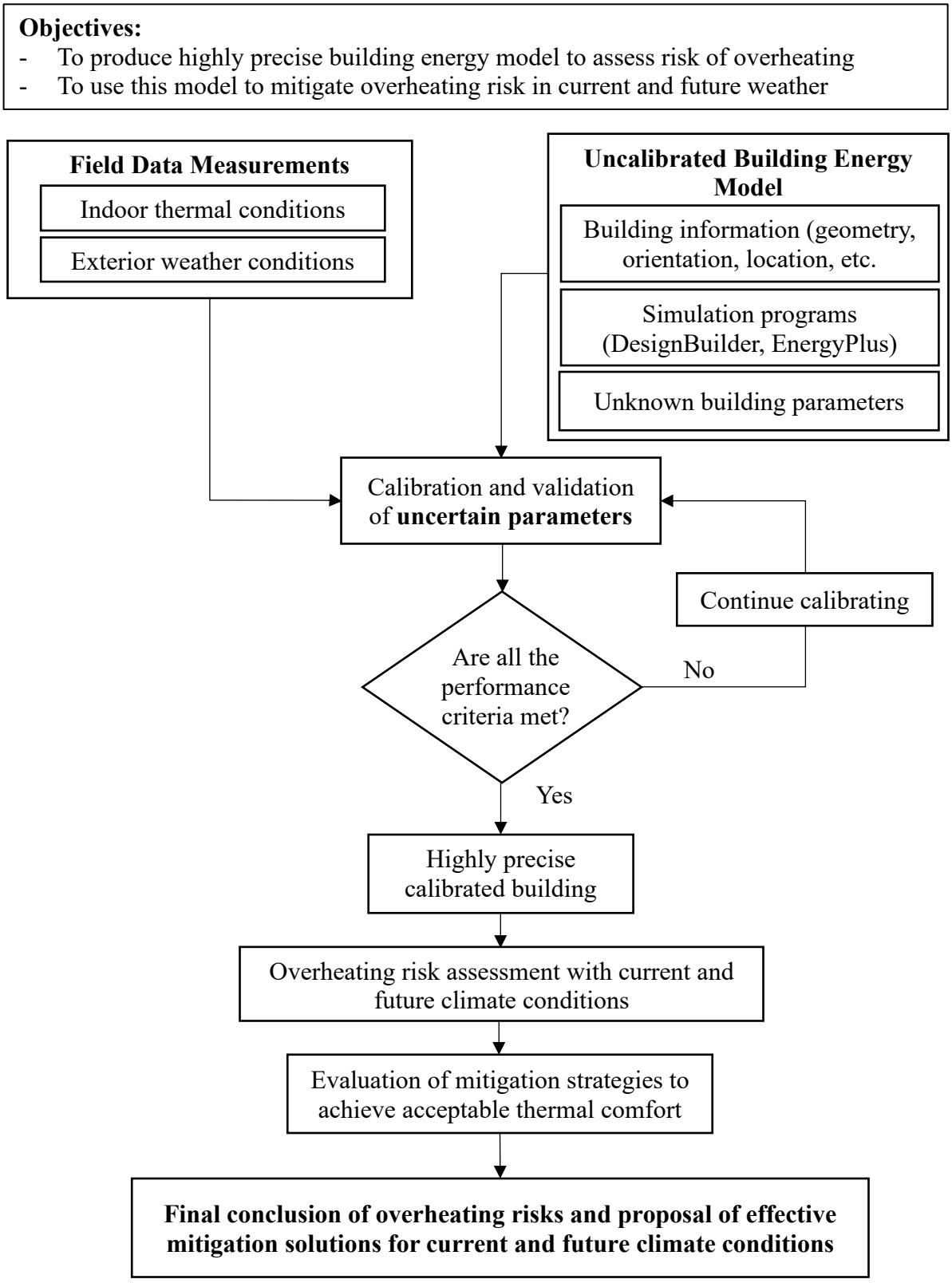

Figure 1. Flowchart of General Calibration Methodology

3.3. Building energy modelling in DesignBuilder

The first step to calibration is the geometry of the building. Using architectural drawings, Google Maps and Google Earth, an approximate model and placement of the building is drawn in DesignBuilder. The architectural plans provide the divisions of the partitions in the building layout. Google Maps, help with the overall building size dimensions, and Google Earth helps with a rough visualization of each model, as well as the building orientation with reference to the north. Additionally, field notes, as collected by the students who install the sensors and collect the data, help with determining the building walls and floor compositions, as well as the window dimensions. The building parameters (envelope materials, window materials, lighting loads, etc.) are inputted into the model. It is these parameters that can then be modified later during calibration. The program can use weather data and building information to simulate results. Once this step is complete, the building model can be exported as an .idf file. This file is then linked to the Bayesian Inference Calibration Code in R Studio or to jePlus for the Multi-Objective Genetic Algorithm.

3.4. Building Parameter Ranges

In both methods used to calibrate building energy models, the same building parameters were used to calibrate each building. Each type (school or hospital) of building had slightly different building parameters.

For the schools, the building parameters used while the school was unoccupied included: wall insulation U-value, window U-value, roof insulation U-value, solar reflectance of window shade rolls, infiltration rate, and solar heat gain coefficient. The building parameters used while the school was occupied included: occupancy, lighting power density, equipment power density, natural ventilation rate, natural ventilation setpoint, and solar reflectance of window shade rolls. The ranges for these building parameters can be found below in Table 1. These values were determined based on similar building types and other existing literature (Baba et al., 2022).

3.5. Sensitivity Analysis

Sensitivity analysis is carried out in both Bayesian Calibration and Multi-Objective Genetic Algorithm. This process is automated using written code in R Studio and Excel spreadsheets and is used to determine building parameters that have the greatest effect on the indoor environment of the building. By ranking the parameters, the focus is then placed on the top 3 to 4 parameters, which are consequently modified to produce the best-calibrated model. And, as mentioned in Chapter 2, the sensitivity analysis calculation that was used for this study is SVI, which is a combination of three commonly used equations, namely SRC value, random forest and t-value.

3.6. Evaluation Criteria Requirements

For all calibration methods, five evaluation criteria items were used. These included RMSE, NMBE, maximum difference between the measured and calibrated hourly indoor air temperature, percentage of calibrated results that were less than 1 degree Celsius away from the measured results and percentage of calibrated results that were less than 0.5 degrees Celsius away from the measured results. In addition to qualitatively observing the trend comparison of temperature over

time graphs between the measured temperatures and the simulated temperature, those five elements provide a quantitative method to determining the accuracy and precision of the simulated results. Hitting the correct target range in all five criteria can confirm how close the building energy model came to matching the actual measured building.

The benchmarks to denote which results were deemed good included a value of less than 0.7 degrees Celsius for the RMSE, a two to three-degree Celsius maximum difference, less than 10 to 15% of the calibrated results more than 1-degree Celsius difference from the measured results and a less than 35 to 50% of the calibrated more than 0.5 degrees Celsius difference from the measured results (Baba et al., 2023). Although there are limited studies on model calibration based on hourly indoor temperature for overheating studies as compared to model calibration for unknown parameters, these target ranges were selected based on existing ranges for evaluation criteria for model calibration from existing literature (Baba, 2022). And so, if the model calibration in this thesis is able to achieve these target ranges, these methodologies will prove to calibrate and assess models for overheating risks with higher accuracy than currently existing methods.

Table 1: Approximate Building Parameter Ranges for Various Building Types in Quebec, Canada

Building Parameters	School (1960s)	School (1990s)	Hospital (1960s)	Residential (1990s)
Wall U-value (W/m^2-K)	0.40 – 0.70	0.10 – 0.40	0.40 – 0.70	0.10 – 0.40
Roof U-value (W/m^2-K)	0.15 – 0.40	0.05 – 0.20	0.23 – 0.33	0.05 – 0.20
Window U-value (W/m^2-K)	2.20 – 3.00	0.75 – 1.50	2.20 – 3.00	0.75 – 1.50
Solar Heat Gain Coefficient	0.45 – 0.75	0.25 – 0.45	0.45 – 0.75	0.25 – 0.45
Window Shade Roll Reflectance (%)	10 - 90	10 - 90	10 - 90	10 - 90
Infiltration Rate (ACH)	0.15 – 0.40	0.05 – 0.15	0.15 – 0.40	0.05 – 0.15
Occupancy (persons/room)	20 – 25	20 – 25	1 – 4	1 – 5
Lighting (W/m^2)	5 – 12	5 – 12	3 – 12	5 – 12
Natural Ventilation Rate (ACH)	0 – 10	0 – 10	0 – 10	0 – 5
Natural Ventilation Setpoint (°C)	21 – 24	21 – 24	21 – 24	21– 24
Equipment Power Density (W/m^2)	2 – 5	2 – 5	2 – 5	2 – 5

3.7. Calibration and Validation Periods

With every building, a calibration and validation period must be chosen. The calibration period refers to the period where the computer model of the building will be modified to be able to output data that matches the measured data from the real building. During this phase, building parameters will be modified as needed and then the model will output simulated data that will be compared to the measured data. Once the differences between the model and the existing building is minimized, the model is calibrated. Then, this now calibrated model will output simulated data over the validation period to be effectively validated, where the simulated output data, using the calibrated model will again be compared to the measured data over the validation period, to see if the calibrated model can adequately simulate the existing building. It is shown that the evaluation criteria of the validation can sometimes have larger degrees of error than the calibration period, but the target range remains the same.

Each period ideally consists of 21 days but can be adjusted depending on the available data, targeted season, and/or any number of reasons that might have affected typical occupant behavior to ensure good results, as was concluded by existing literature (Baba, 2022). A minimum of 14 days and a maximum of 28 days is required for calibration, while 21 to 28 days is required for validation. This is based on the assumption that 14 days is the minimum required time period to observe a regularity in occupant movements and patterns; and that 28 days would be the limit of where significant changes in occupant habits may appear.

3.8. Unoccupied and Occupied Calibration Periods for School Buildings

In both methods, the buildings must be calibrated without occupants and then that calibrated building model is used as the starting point for the calibration of the model with occupants. This allows the calibration of only the building envelope at first, focusing on the building's physical properties that will not change once the building is occupied. These parameters include the wall insulation U-value, roof insulation U-value, window U-value, window SHGC, air infiltration and window shading. In this case, parameters related to an occupied building including occupancy, lighting loads, equipment loads and natural ventilation (no one is there to open or close the windows) are set to zero. Once the building envelope is calibrated while unoccupied, those parameters will not change during the calibration during the occupied period. And so, the parameters related to internal loads and occupant-dependent properties (opening and closing of windows and shades, internal loads, etc.) that were originally set to zero will be turned on to calibrate the building with occupants.

This process only exists for the school buildings, as the schools are considered closed during the summer (July-August). The hospital and residential buildings are occupied year-round, therefore both the building envelope and occupant-related parameters must be calibrated simultaneously.

4. Comparison of Bayesian Inference and MOGA Calibration

In this section, the two described methods for calibrating building models will be discussed below. While both methods have been successful in achieving precise models, they have achieved this through a similar process that is described in the next section. Both methods were applied to one of the schools to compare the precision of the calibration results. In the end, while both methods achieved high precision results as compared to existing calibration methods, the multi-objective genetic algorithm (MOGA) method was able to achieve better results in calibrating multiple individual rooms simultaneously. Ultimately, after the calibration of this school, the rest of the buildings in this thesis were calibrated using the MOGA method.

4.1. Computing Time Differences between Calibration Methods

Multi-objective genetic algorithm (MOGA) has been able to achieve similar or higher precision than Bayesian calibration with less computing power. While Bayesian is very good for calibrating a building with the use spatial averages, which computes an average temperature for the entirety of the building, based off of a few calculated rooms, and has a quicker set-up compared to MOGA, the computing time is significantly longer as it runs through 20 000 iterations to then take the average value of these iterations to produce the final calibrated values. This process is considerably quick with the amount of data it must produce, but it is not yet capable of producing a higher level of precision, as calculated by the performance criteria targets, than MOGA when observing individual rooms' calibration results. On the other hand, MOGA takes more time to set up the parameter ranges and connect the necessary computer codes and software programs, but the computing time is much quicker and can accurately calibrate multiple rooms simultaneously. The MOGA method only goes through a maximum of 10 generations of Pareto-optimal solutions for a total of 100 iterations before producing a set of calibrated building parameters.

4.2. Bayesian Calibration of School 1

This is the first and only school that was calibrated using Bayesian Inference and MOGA calibration methods.

4.2.1. Building description of School 1

School 1 is a two-storey primary school in Montreal, Quebec, Canada. Four rooms on the top floor were selected for the study, with the installation of indoor temperature sensors in each room and a weather station that was installed on the roof. It was built in 1958 and features a red brick façade, double pane windows, interior shade rolls and approximately 60% window-to-wall ratio. There is no mechanical cooling, therefore it relies on natural ventilation with windows that have an openable area of 25%.

Figure 2: Google Streetview of School 1

4.2.2. Building energy model

With this building and all buildings to follow, the basic geometry and measurements of the school were created in DesignBuilder. Using this software, buildings can be created in a 3D space using approximate dimensions, window-to-wall ratio and geographic orientation of the existing building. These building elements are integrated in DesignBuilder based on the information that is available per building, by using a combination of building plan measurements and Google Earth's and Google Maps' measuring tools are used. All building properties are also added, including window, wall and roof properties, natural ventilation rates, ventilation setpoints, occupancy, lighting and equipment loads, infiltration rates, etc. These properties are initially added based on existing literature ranges, before fully calibrating them, as shown in Table 1. For natural ventilation, this is modelled in DesignBuilder by adjusting the window opening area and the Airflow Network calculations performed by EnergyPlus that is integrated in this program. As much information as possible is included based on known building details, scheduling and function are included to facilitate the calibration process. These parameters can then be adjusted during the calibration process to later use the calibrated building model to assess for overheating risk and run building simulations to evaluate mitigation techniques, while also using current and future weather data files.

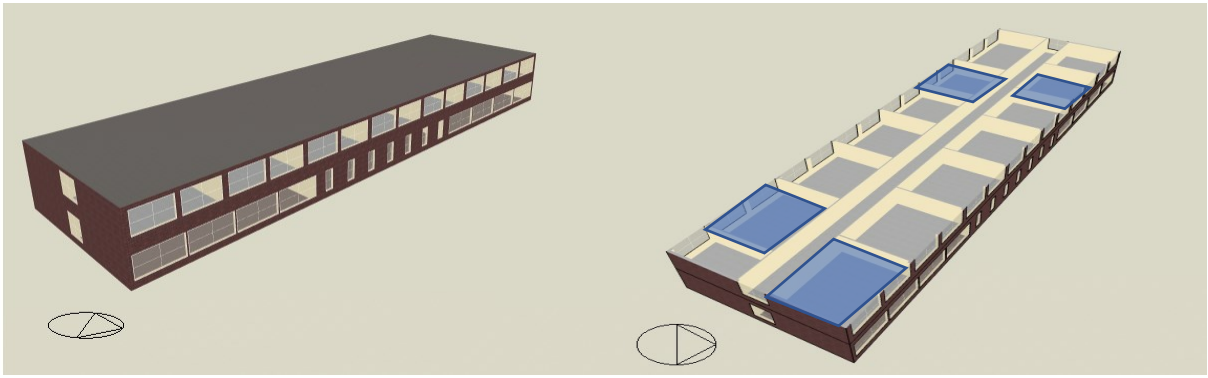

Figure 3: Renderings of School 1 in DesignBuilder

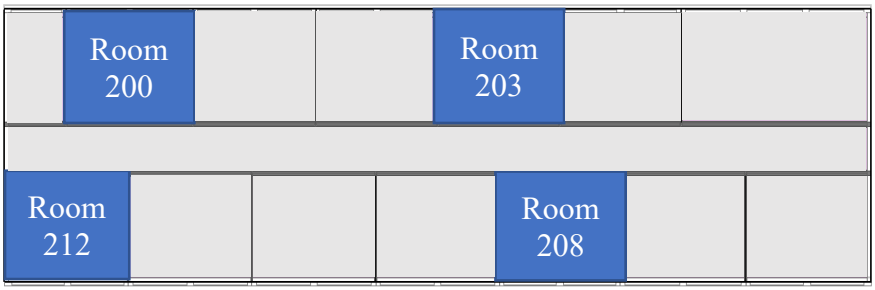

Figure 4: Plan view of School 1 with the measured rooms identified

4.2.3. Calibration results using Bayesian Calibration for School 1

For this school, the calibration process is performed on the building when it is unoccupied and again when it is occupied. The building is first calibrated for a time period for which the school was closed from May 23 to June 3, 2020, using building parameters that are specific to the building envelope and excluding any parameters related to building occupants. Following the calibration of the unoccupied building, this calibrated model was then used as the starting point to begin the calibration of the occupied building using parameters that are affected by the occupants, such as the opening of windows, the use of shades on windows, the use of lights and equipment, etc. Using the calibrated unoccupied model, all 6 steps are repeated using the occupied building parameters.

It is important to highlight that in Step 4, separate meta-models are generated for each measured room after the building has been evaluated as a whole during the parametric simulation and the sensitivity analysis. Therefore, there are 4 separate calibrated meta-models that were used to for each individual room. While each meta-model started from the same file, each file was then calibrated according to the field measurements that were provided for each room to ultimately produce 4 calibrated meta-models. This allows for the calibrated values to be output based on the specific input measurements from each individual measured room. The way this is applied in the unoccupied case and the occupied case is different as explained below.

In the case of the unoccupied building calibration, the final calibrated model used the average of the calibrated values calculated from each individual room for parameters that must be the same throughout the whole building. For example, the average was taken for wall insulation thickness, roof insulation thickness, infiltration rate from the four measured rooms, however each room's percentage of the shade covering the window of that room was applied as it was calculated by that specific room's data. In short, room level calibrated building parameters were used as calculated in the final calibrated model, while building level calibrated parameters were calculated from the average of the values that had resulted from the room specific calibrations.

In the case of the occupied building calibration, the final calibrated model uses a combination of all the room-level calibrated parameters. First, the average of each building parameter is applied to all the building zones, and then the room specific calibrated values are applied to those individual rooms and the surrounding rooms. As a result, the final calibrated model will have the values as calculated according to room level data all in one model.

The figure below shows the difference in simulated results using the calibrated model compared to the collected data from the indoor sensors. The orange line represents the calibrated building model indoor temperature, while the blue line represents the measured indoor temperature data. The following tables present the calibrated building parameters used in the calibrated model and quantify the errors between measured and simulated data using performance criteria.

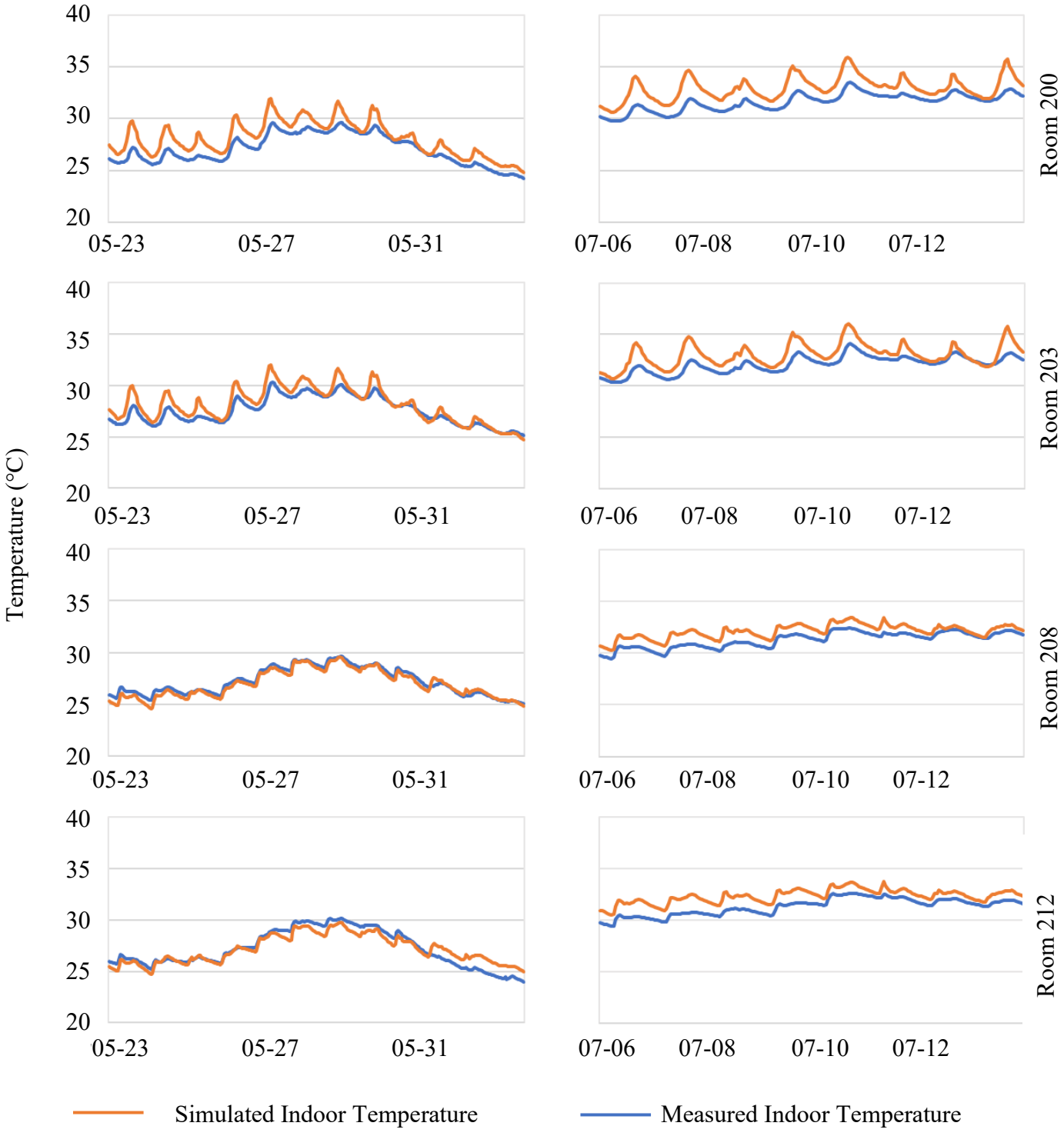

Figure 5: Comparison of the indoor temperature of each classroom using the calibrated model and the collected data during the unoccupied period at School 1

Table 2: Calibrated building parameters during the unoccupied period for School 1 using Bayesian Inference

Parameters	R 200	R 203	R 208	R 212
Shading solar reflectance	0.7	0.6	0.4	0.4
Infiltration Rate (ACH)			0.16	
Wall Insulation U-value (W/m2-K)			0.46	
Roof Insulation U-value (W/m2-K)			0.27	

This first table shows the values of the important (as determined by the sensitivity analysis) unknown parameters calibrated using Bayesian Inference to create a building model in which its simulated indoor temperatures are very closely matched to the measured results of this building. The difference between these sets of data is measured by the evaluation criteria in Table 3. The RMSE measures the average differences between the measured and simulated results. A target of 0.7°C was set for the RMSE value to achieve a high level of precision with the model. Normalized Mean-Bias Error (NMBE) was also used to evaluate the error as it is a typical indicator in calibration statistics. However, it was not a limiting factor in this study. The maximum difference, which is an indicator of the maximum difference between the simulated and measured results at any given hour during the calibration period, and RMSE were often the indicators that did not meet their targets during initial rounds of calibration. The final two indicators calculate the percentage of the simulated data set in which the difference from the measured data set is more than 1°C or more than 0.5°C, with targets of 15% and 50%, respectively. In this case, the calibration of R 200 was not able to achieve the above-mentioned goals. This can be explained by unknown field situations, such as unexpected occupancy when the building was supposed to be closed, lights that were left on by accident, windows that were left open, rolling blind shades that were left open, etc. However, using the results from the other three rooms to determine the building envelope parameters, the calibration process continued with the next step of calibrating the building while occupied to calibrate the occupancy-related parameters such as natural ventilation, lighting, number of occupants, percentage of shade roll opening, etc.

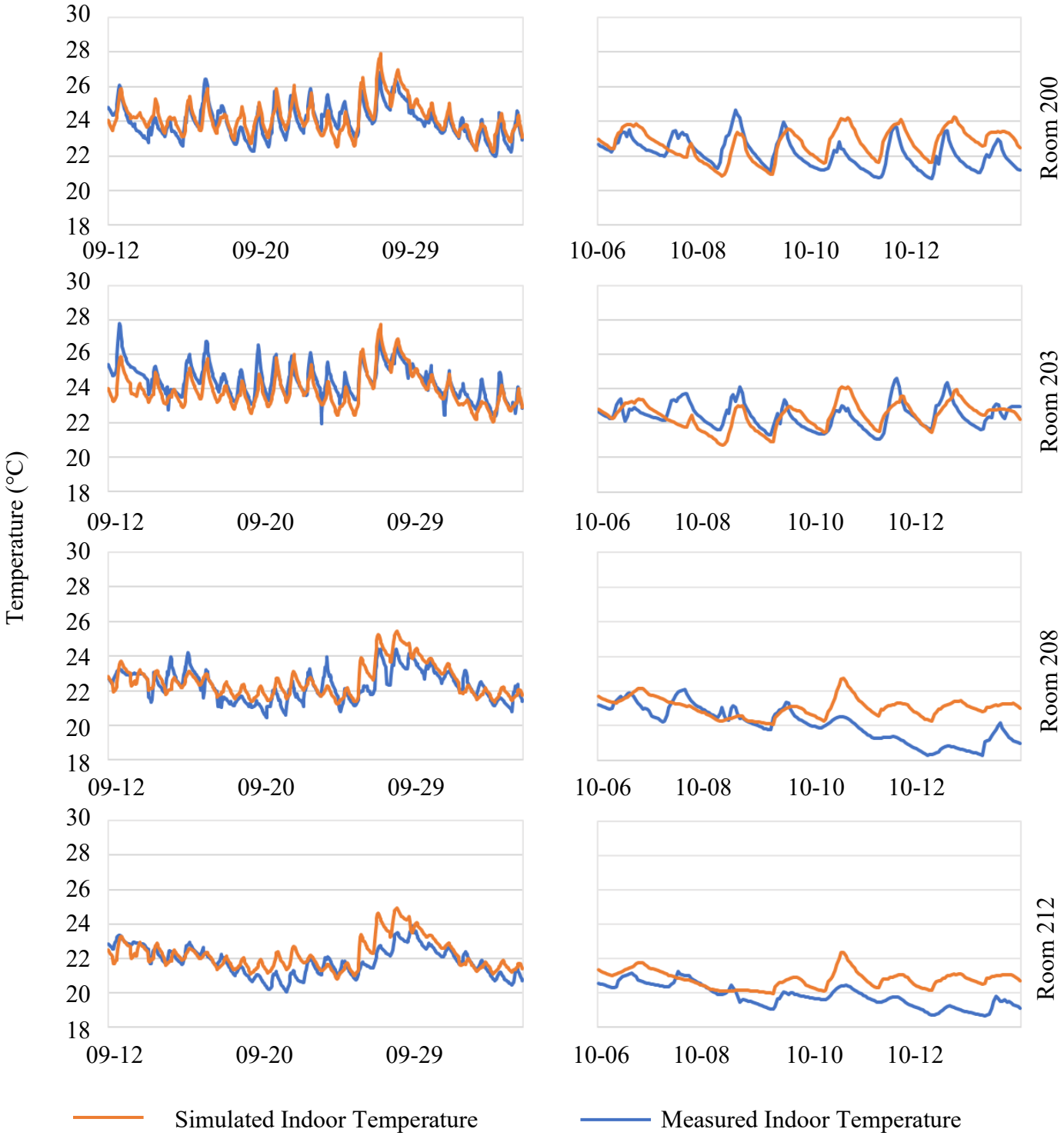

Figure 6: Comparison of the indoor temperature of each classroom using the calibrated model and the collected data during the occupied period at School 1

Table 3: Evaluation criteria during the calibration and validation period using the calibrated model during the unoccupied period for School 1 using Bayesian Inference

Evaluation criteria	Calibration				Validation			
	R 200	R 203	R 208	R 212	R 200	R 203	R 208	R 212
RMSE (ºC)	1.2	0.8	0.4	0.7	1.3	1.0	0.6	0.8
NMBE (%)	3.8	2.0	-0.8	-0.1	3.4	2.4	1.5	2.4
Max Diff. (ºC)	2.8	2.2	1.0	1.4	3.6	3.0	1.7	1.8
1 °C Percentage Error (%)	33	14	0	7	51	22	2	16
0.5 °C Percentage Error (%)	74	38	3	35	69	50	28	50

Table 4: Calibrated building parameters during the occupied period for School 1 using Bayesian Inference

Parameters	R 200	R 203	R 208	R 212
Max NV amount (ACH)	7.5	5.7	7.7	7.8
NV setpoint (ºC)	23.7	22.7	21.1	21.0
Maximum lighting load (W/m^2)	9.1	9.1	9.1	9.1
Shading solar reflectance	0.86	0.89	0.57	0.86

Table 5: Evaluation criteria during the calibration and validation period using the calibrated model during the occupied period for School 1 using Bayesian Inference

Evaluation criteria	Calibration				Validation			
	R 200	R 203	R 208	R 212	R 200	R 203	R 208	R 212
RMSE (ºC)	0.6	0.8	0.7	0.7	1.1	0.9	1.4	1.1
NMBE (%)	0.9	-2.0	1.2	1.7	2.6	0.3	4.7	4.7
Max Diff. (ºC)	1.4	2.5	2.0	2.1	2.3	2.7	2.8	2.1
1 °C Percentage Error (%)	3	10	7	15	33	14	45	36
0.5 °C Percentage Error (%)	30	37	32	31	61	39	57	68

4.3. Calibration Results using MOGA for School 1

The following results are produced using MOGA mainly through the software jePlus. This software provides the framework for calibrating many significant parameters simultaneously until a set of optimal solutions are achieved. A python script developed by Baba et al. is also used in combination with this software to evaluate the performance of these solutions. Once a set of optimized values is achieved, these sets are then inserted into DesignBuilder to calibrate the base model. This process only requires one meta-model, because all 4 rooms are calibrated simultaneously. The following tables list the results of the calibration over the same time period as the Bayesian calibration method using MOGA method.

Table 6: Calibrated building parameters during the unoccupied period for School 1 using MOGA

Parameters	**R 200**	**R 203**	**R 208**	**R 212**
Shading solar reflectance	0.50	0.60	0.60	0.40
Infiltration Rate (ACH)	0.18			
Wall Insulation U-value (W/m^2-K)	0.41			
Roof Insulation U-value (W/m^2-K)	0.21			

Table 7: Evaluation criteria during the calibration and validation period using the calibrated model during the unoccupied period for School 1 using MOGA

Evaluation criteria	**Calibration**				**Validation**			
	R 200	**R 203**	**R 208**	**R 212**	**R 200**	**R 203**	**R 208**	**R 212**
RMSE (ºC)	0.4	0.5	0.3	0.7	0.6	0.6	0.6	0.9
NMBE (%)	0.0	-0.1	-0.4	0.4	-0.3	0.2	1.5	2.5
Max Diff. (ºC)	1.2	1.2	0.9	1.7	1.7	2.1	1.7	1.8
1 °C Percentage Error (%)	2%	2%	0%	20%	11%	9%	7%	31%
0.5 °C Percentage Error (%)	26%	29%	9%	41%	38%	35%	44%	72%

Table 8: Calibrated building parameters during the occupied period for School 1 using MOGA

Parameters	R 200	R 203	R 208	R 212
Shading solar reflectance	0.90	0.90	0.80	0.90
Maximum lighting load (W/m^2)	6.00	6.00	6.00	6.00
NV setpoint (ºC)	23.00	23.00	21.00	20.00
Max NV amount (ACH)	9.00	9.00	9.00	9.00

Table 9: Evaluation criteria during the calibration and validation period using the calibrated model during the occupied period for School 1 using MOGA

Evaluation criteria	Calibration				Validation			
	R 200	R 203	R 208	R 212	R 200	R 203	R 208	R 212
RMSE (ºC)	0.6	0.8	0.7	0.7	1.1	0.9	1.4	1.1
NMBE (%)	0.9	-2.0	1.2	1.7	2.6	0.3	4.7	4.7
Max Diff. (ºC)	1.4	2.5	2.0	2.1	2.3	2.7	2.8	2.1
1 °C Percentage Error (%)	11%	19%	14%	19%	50%	21%	49%	43%
0.5 °C Percentage Error (%)	51%	53%	44%	42%	74%	58%	66%	80%

4.4. Summary

In this section, the values obtained by calibrating the school building using Bayesian calibration and multi-objective genetic algorithm are compared side by side to highlight the differences of each method's calibrated values. In addition to a slightly higher accuracy as determined by the evaluation criteria using the MOGA method, this process only required one meta-model per building (as opposed to a using one meta-model per room when using Bayesian calibration), was able to calibrate multiple rooms simultaneously to produce one final calibrated model and used less computing time with less iterations to find the optimal solution.

Table 10: Comparison of calibrated parameters during the unoccupied period using Bayesian Calibration and Multi-objective Genetic Algorithm

Building Parameter	R 200		R 203		R 208		R 212		Difference
	BC	MOGA	BC	MOGA	BC	MOGA	BC	MOGA	
Shading solar reflectance	0.70	0.50	0.60	0.60	0.40	0.60	0.40	0.40	0 – 0.2
Infiltration Rate (ACH)	0.16	0.18	0.16	0.18	0.16	0.18	0.16	0.18	0.2
Wall U-value (W/m^2-K)	0.46	0.41	0.46	0.41	0.46	0.41	0.46	0.41	0.05
Roof U-value (W/m^2-K)	0.27	0.21	0.27	0.21	0.27	0.21	0.27	0.21	0.06

Table 11: Comparison of calibrated parameters during the occupied period using Bayesian Calibration and Multi-objective Genetic Algorithm

Building Parameter	R 200		R 203		R 208		R 212		Difference
	BC	MOGA	BC	MOGA	BC	MOGA	BC	MOGA	
Shading solar reflectance	0.86	0.90	0.89	0.90	0.57	0.90	0.86	0.90	0.04 – 0.33
Max lighting load (W/m^2)	9.10	6.00	9.10	6.00	9.10	6.00	9.10	6.00	3.10
NV setpoint (°C)	23.70	23.00	22.70	23.00	21.10	23.00	21.00	23.00	0.03 – 2.00
Max NV (ACH)	7.50	9.00	5.70	9.00	7.70	9.00	7.80	9.00	1.20 – 3.30

For calibrated building envelope parameters, the values obtained by both methods differ by less than a tenth. The differences between calibrated building parameter values are larger in occupant-dependent parameters, which is to be expected because occupant behavior can change quickly and without notice. Such behaviors can include forgetting to close the windows and/or lights at the end of the day, changes in window-opening patterns and/or use of shade rolls depending on daily activities and/or changes in weather, etc.

Table 12: Comparison of evaluation criteria while unoccupied using Bayesian Calibration and Multi-objective Genetic Algorithm during the calibration period

Evaluation Criteria	R 200*		R 203		R 208		R 212		Difference
	BC	MOGA	BC	MOGA	BC	MOGA	BC	MOGA	
RMSE (°C)	1.2	0.4	0.8	0.5	0.4	0.3	0.7	0.7	0 – 0.3
NMBE (%)	3.8	0.0	2.0	-0.1	-0.8	-0.4	-0.1	0.4	0.4 – 2.1
Max Diff. (°C)	2.8	1.2	2.2	1.2	1.0	0.9	1.4	1.7	0.1 – 1.0
Greater than 1°C Error (%)	33	2	14	2	0	0	7	20	0 – 13
Greater than 0.5°C Error (%)	74	26	38	29	3	9	35	41	6 – 9

**Room 200 was not successfully calibrated according to the target ranges. Therefore, it was excluded in the calculations for the difference in values between BC and MOGA*

Table 13: Comparison of evaluation criteria during the occupied period using Bayesian Calibration and Multi-objective Genetic Algorithm during the calibration period

Evaluation Criteria	R 200		R 203		R 208		R 212		Difference
	BC	MOGA	BC	MOGA	BC	MOGA	BC	MOGA	
RMSE (°C)	0.6	0.6	0.8	0.8	0.7	0.7	0.7	0.7	0
NMBE (%)	0.9	0.9	-2.0	-2.0	1.2	1.2	1.7	1.7	0
Max Diff. (°C)	1.4	1.4	3.5	2.5	2.0	2.0	2.1	2.1	0 – 1.0
Greater than 1°C Error (%)	3	11	10	19	7	14	15	19	4 – 8
Greater than 0.5°C Error (%)	30	51	37	53	32	44	31	42	11 – 21

In conclusion, although there were very many similarities in processing times, ease of use and precision of results between the two methods, MOGA method was slightly better adapted to perform the task at hand. As shown in Tables 12 and 14, the RMSE value was often less than that attained by BC by several tenths of a degree Celsius. MOGA was also able to successfully calibrate all 4 rooms of the building in all cases. The maximum difference calculated using MOGA was also less than that calculated by BC by up to 1°C. The Bayesian calibration method was a robust automatic calibration method that was better suited to calibrate buildings as a whole, but was not as effective as MOGA to calibrate individual rooms simultaneously. The set-up time for both methods have its advantages and disadvantages with comparable ease of use. Even though the Bayesian calibration platforms were less user-friendly and more heavily reliant on the user's

knowledge of programming code, this design also allowed for easier access to code customization and troubleshooting. On the other hand, MOGA had an easier to understand user interface, although getting access to the program code for troubleshooting was a bit more complex. And so, after evaluating both methods, the rest of the school building models, residential building models and hospital building models that were calibrated in this paper will use MOGA method from this point forward. The following three school models also used the calibrated School 1 model's building parameters as a baseline for their calibration.

5. Calibration using the MOGA Method for existing Canadian Buildings

After completing the calibration of School 1 using both Bayesian Inference Calibration method and Multi-Objective Genetic Algorithm methods, a set of building parameter ranges were found. All the schools that were assessed in this thesis were built around the same time and are similar in structure and function. Therefore, the same building parameter ranges obtained from School 1, were used to calibrate the subsequent three schools using automatic calibration with DesignBuilder. After modeling each building in DesignBuilder, the unknown parameters were modified with each simulation and then the simulation results are exported to an Excel sheet, where the evaluation criteria can be calculated and the differences between the measured and calibrated data can be compared. The results of this process for the three additional schools are shown in the following sections. This process was also used to calibrate a hospital and residential building. However, the parameter ranges for these buildings were obtained from typical building ranges and building codes. All the buildings that were calibrated for this thesis are shown in the Figure 7. The school buildings are shown in yellow; the hospital building is shown in red; and the residential building is shown in green.

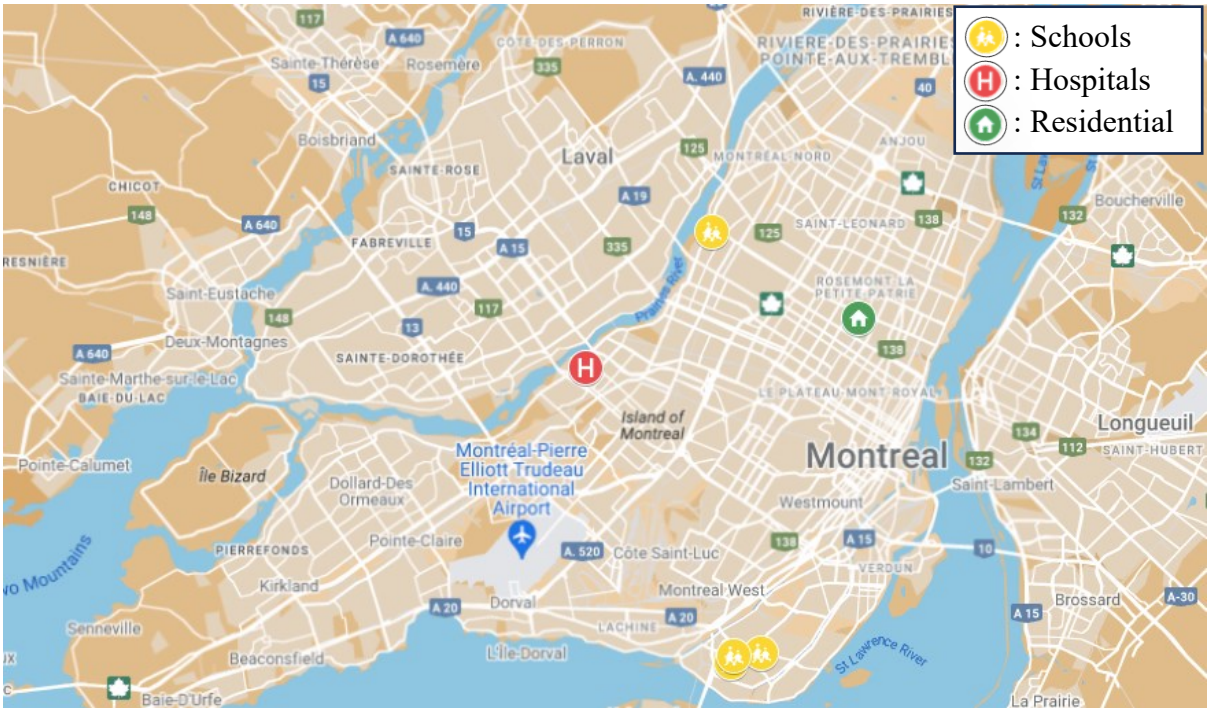

Figure 7: Calibrated Buildings Identified on a Map of Montreal (Google Maps)

5.1 Calibration of School Buildings

This thesis investigated the calibration of four school buildings built in 1950s to 1960s. Here is a summary of general building characteristics for all school buildings.

Table 14: Major building features of calibrated school buildings

Building Parameters	School 1	School 2	School 3	School 4
Year of Construction	1958	1958	1960	1953
Major Renovations (building additions)	N/A	1990s and 2000s	unknown	1990s
Building Shape	Rectangular	C-shaped (only calibrated original rectangular building)	Irregular	T-shaped (originally rectangular before the additions)
Number of Storeys	2	2	1	2
Wall Materials	Red brick veneer, concrete block	Yellow brick veneer, concrete block	Red brick veneer, concrete block (except one kindergarten room)	Yellow brick veneer, concrete block
Window Composition	Double windows with single glass	Double windows with single glass	Double windows with single glass	Double windows with single glass
Window-to-Wall Ratio	60%	30-40%	20%	30-40%
Window Opening Area	25%	25%	10-20%	20-30%
Interior Shading	Rolling shades	Rolling shades	Rolling shades	Rolling shades
Ventilation	Natural	Natural	Natural	Natural and mechanical (in select rooms, no air cooling)

Using these building details, in combination with provided architectural plans, the building models are created in DesignBuilder. The geometry and building orientation are created from the architectural plans and then the building envelope properties and occupancy loads are entered as input parameters. These inputs are important in creating the baseline building before starting calibration. In DesignBuilder, the specific inputs included wall u-value, roof u-value, window u-value, solar heat gain coefficient, infiltration rate, solar reflectance of shade rolls, natural ventilation rate and setpoint, number of occupants, lighting loads, and equipment loads.

School 2

Figure 8: Aerial view of School 2 from Google Earth

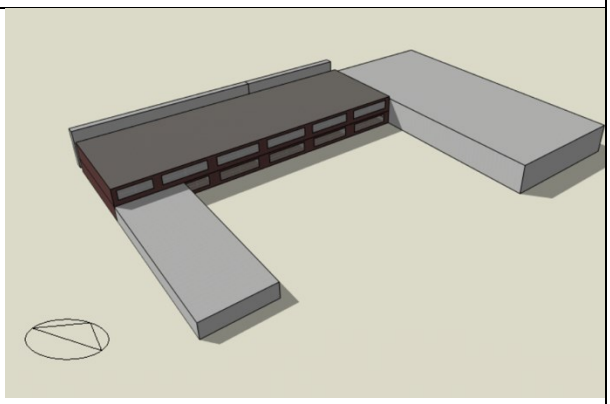

Figure 9: Axonometric view of the building energy model in DesignBuilder of School 2

School 3

Figure 10: Google Earth view of School 3

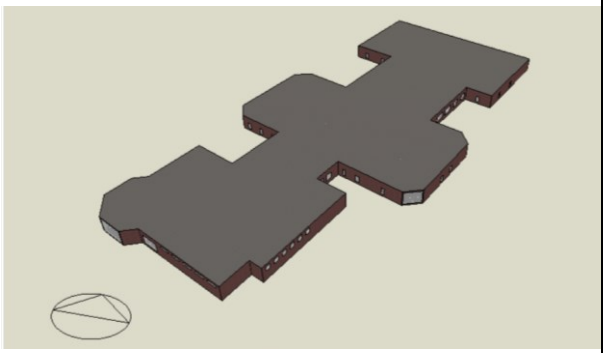

Figure 11: Axonometric View of School 3 in DesignBuilder

School 4

Figure 12: Google Earth View of School 4

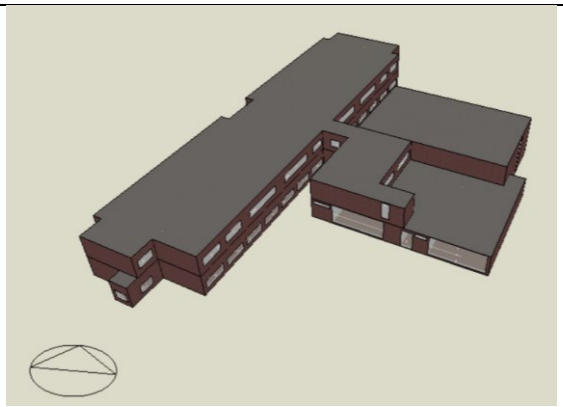

Figure 13: Axonometric View School 4 in DesignBuilder

In some cases, only the main building or a section of the building where the monitored rooms are located are modelled in detail with room partitions and the surrounding buildings and/or trees are modelled as adjacent blocks. It is done this way to save on computing time, while still considering the surrounding environment. These adjacent blocks are shown in grey in Figure 9 above. There are four rooms per school that were equipped with temperature sensors. School 2 had two measured rooms on the top floor and two measured rooms on the bottom floor. School 3 is only one-storey high and had 4 measured classrooms, including one kindergarten room that acts more like an activity room. School 4 had two measured rooms in the top floor of the original construction and two measured rooms on the first floor in the building addition from 1990s. For further details concerning the plan views of School 3 and School 4, please see Chapter 9.

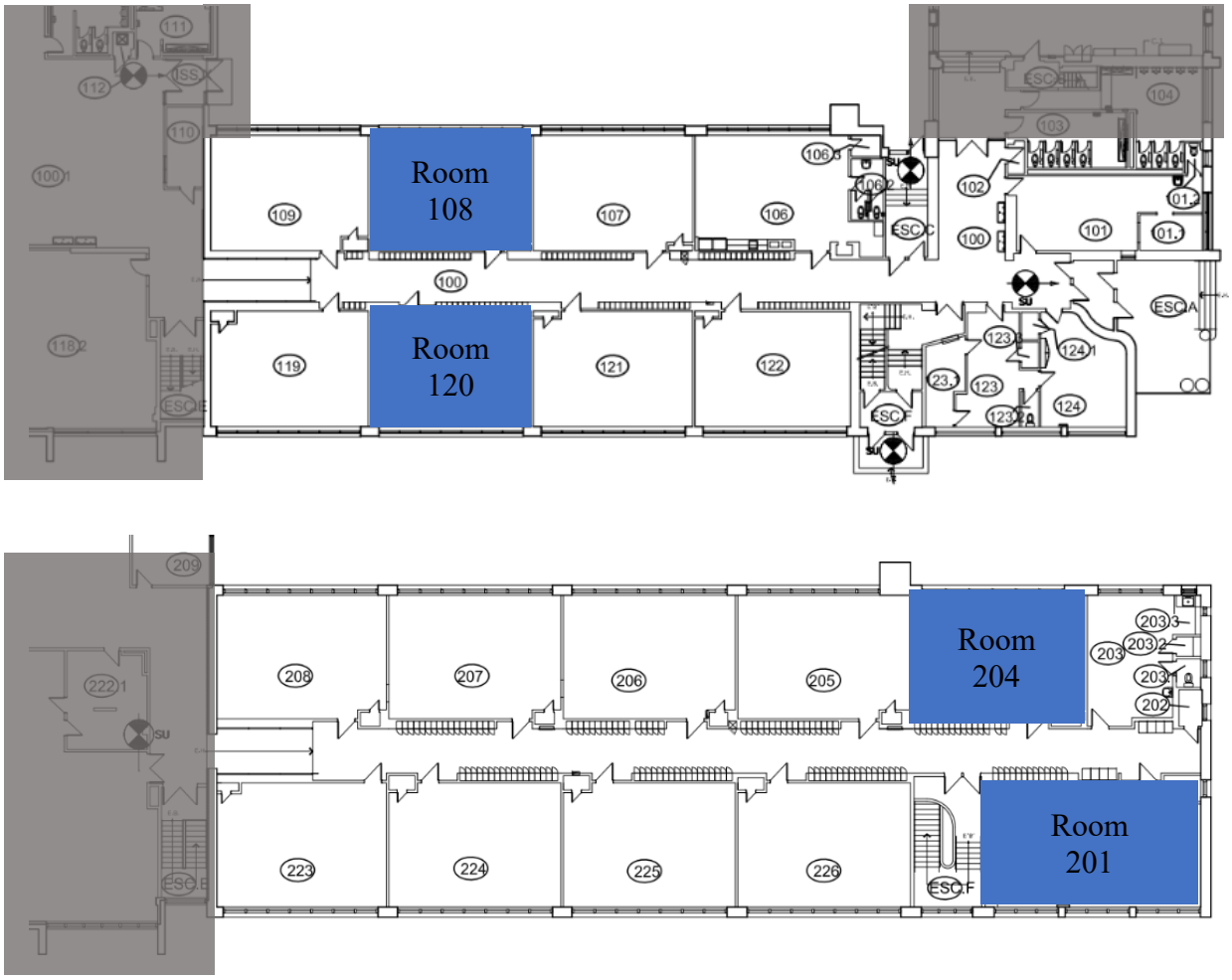

Figure 14: Plan view School 2 of first floor (top) and second floor (bottom)

For the school cases, the calibration process was performed in two steps. First, each building was calibrated during the summertime months when the building is expected to be empty. A period of 3 weeks during the months of July and/or August was chosen for the calibration step and another 2 to 3 weeks directly following the calibration period was chosen for the validation step. This two-step process was required to first calibrate the building envelope's parameters without any occupancy loads. These parameters included the building wall U-value, roof U-value, window U-

value and SHGC, air infiltration rate and solar reflectance of rolling shades percentage. Once these values are calibrated, the next step is to keep those parameters constant while then including occupancy loads, such as lighting power density, equipment power density, number of occupants per room, natural ventilation rate and setpoint and again solar reflectance of rolling shades percentage.

While there are 6 parameters to adjust during the calibration process, some parameters have a greater effect on the simulation output than others. For example, when the school is occupied, the most important parameters included natural ventilation rate and solar reflectance of rolling shades. Increasing the fraction of solar reflectance led to decreasing the indoor temperature and increasing natural ventilation during the cooler parts of the day (early morning and at night) led to decreasing indoor temperatures. Equipment power density had the smallest effect on the indoor temperature simulation results. However, increasing the number of occupants could significantly increase the indoor temperature during the day. Similarly, but to a lesser extent, increasing lighting power density during the day also increased indoor temperature, but more notably adding or removing lighting during the night had a significant effect in proper calibration of the simulation results. Therefore, inputting the correct scheduling is a very important input in the calibration process.

With each step of the calibration process, the resulting calibrated values of these parameters are evaluated using 5 evaluation criteria: RMSE, NMBE, maximum hourly difference, percentage of hourly differences that were below 1°C and percentage of hourly differences that were below 0.5°C. The degree differences are taken from the difference between the simulated result generated by the calibrated model compared to the measured result collected from the sensor. The target range for these performance metrics was determined by selecting a range that would yield a more accurate calibrated model, compared to the existing standards required by ASHRAE (Baba et al., 2022b). Therefore, by meeting these targets, the calibration methodology produced calibrated models that are well below the current standards required by ASHRAE (Baba et al., 2022b). The same evaluation criteria were used for all building types (school, hospital, residential).

Table 15: Target ranges for evaluation criteria

Evaluation Criteria	Target Range
RMSE (°C)	Less than 0.70 °C
NMBE (%)	Less than +/- 5.0%
Maximum Hourly Difference (°C)	2 to 3 °C
Percentage of Hourly Differences below 1°C	Less than 15%
Percentage of Hourly Differences below 0.5°C	Less than 50%

5.1.1. Comparison of Calibration Results for School Buildings

Overall, all four schools were built around the same year and fulfill the same building function, and therefore have similar building envelope parameters and occupancy parameters.

5.1.1.1. Calibration results for School 2

The calibration for School 2 was successful for all four rooms as is shown in Table 17 and 19. This building was the most like School 1 compared to the other three schools. Both schools were rectangular with two floors, however two of the measured rooms were on the second floor and two of the measured rooms were on the first floor for School 2. All rooms were approximately the same size and had the same function.

Table 16: Calibrated building parameters during the unoccupied period for School 2

Parameters	R 108	R 120	R 201	R 204
Shading solar reflectance	0.65	0.80	0.50	0.60
Air infiltration Rate (ACH)	0.25			
Wall insulation U-value (W/m^2-K)	0.38			
Roof insulation U-value (W/m^2-K)	0.23			

Table 17: Evaluation criteria results during the unoccupied period for School 2

Evaluation criteria	Calibration				Validation			
	R 108	R 120	R 201	R 204	R 108	R 120	R 201	R 204
RMSE (ºC)	0.8	0.6	0.6	0.7	0.5	0.4	0.8	0.6
NMBE (%)	0.1	1.5	0.5	-0.3	-1.0	0.9	1.9	0.8
Max diff. (ºC)	2.2	1.5	2.4	2.0	2.0	1.2	2.5	2.8
1 °C percentage error (%)	18%	10%	12%	9%	9%	2%	20%	8%
0.5 °C percentage error (%)	56%	43%	34%	44%	34%	18%	48%	26%

Table 18: Calibrated building parameters during the occupied period for School 2

Parameters	R 108	R 120	R 201	R 204
Max NV amount (ACH)	7.60	7.60	7.60	7.60
NV setpoint (ºC)	21.20	21.20	21.20	21.20
Maximum lighting load (W/m^2)	9.00	9.00	9.00	9.00
Shading solar reflectance	0.40	0.85	0.90	0.70

Table 19: Evaluation criteria results during the occupied period for School 2

Evaluation criteria	Calibration			
	R 108	R 120	R 201	R 204
RMSE (ºC)	0.7	0.9	0.5	0.6
NMBE (%)	-0.8	-0.1	0.4	0.2
Max diff. (ºC)	2.9	3.8	1.8	2.8
1 °C percentage error (%)	11%	21%	5%	6%
0.5 °C percentage error (%)	47%	53%	32%	25%

Validation was not performed on this school, because the results were already validated with the previous school.

5.1.1.2. Calibration results for School 3

During the calibration of this school, one of the rooms (Room 60), which was a classroom for school children under the age of 6, could not be calibrated. Its building materials are unknown, and its function is also different. This room functions as an activity room, and the children in this room likely move around more than the children in the other classrooms. The windows are also a lot larger, and it is unclear if there may be mechanical ventilation. The other three measured rooms were successfully calibrated, achieving less than 0.8°C RMSE and less than 15% of the calibrated results had a less than 1°C difference than the measured results. The calibrated parameters of this first phase of calibration where the building was unoccupied, is then used to calibrate the school while it was occupied. And again, the calibrated results were evaluated against the performance metrics to conclude the calibration results are accurate as shown in Table 21.

Table 20: Calibrated building parameters during the unoccupied period for School 3

Parameters	R 14	R 23	R 34	R 60
Shading solar reflectance	0.90	0.30	0.50	0.50
Air infiltration Rate (ACH)	0.25			
Wall insulation U-value (W/m^2-K)	0.40			
Roof insulation U-value (W/m^2-K)	0.20			

Table 21: Evaluation criteria results during the unoccupied period for School 3

Evaluation criteria	Calibration				Validation			
	R 14	R 23	R 34	R 60	R 14	R 23	R 34	R 60

RMSE (ºC)	0.6	0.6	0.7	1.9	0.4	0.7	0.8	1.9
NMBE (%)	1.0	-1.2	-1.3	-5.4	0.3	-2.5	-1.8	-4.9
Max diff. (ºC)	1.8	1.3	1.7	3.3	1.3	1.7	1.9	3.0
1 °C percentage error (%)	8%	8%	14%	73%	3%	17%	33%	75%
0.5 °C percentage error (%)	37%	40%	52%	86%	52%	55%	54%	90%

Table 22: Calibrated building parameters during the occupied period for School 3

Parameters	**R 14**	**R 23**	**R 34**	**R 60**
Max NV amount (ACH)	3.00	7.00	7.00	2.00
NV setpoint (ºC)	22.00	22.00	22.00	22.00
Maximum lighting load (W/m^2)	9.00	9.00	9.00	9.00
Shading solar reflectance	0.90	0.30	0.80	0.30

Table 23: Evaluation criteria results while occupied for School 3

Evaluation criteria	**Calibration**				**Validation**			
	R 14	**R 23**	**R 34**	**R 60**	**R 14**	**R 23**	**R 34**	**R 60**
RMSE (ºC)	0.6	0.7	0.6	1.1	1.6	2.7	0.9	1.8
NMBE (%)	1.5	-2.3	-1.1	-0.5	-4.7	-12.4	-1.8	-5.3
Max diff. (ºC)	1.9	2.7	2.2	3.5	4.7	5.0	2.9	3.5
1 °C percentage error (%)	11%	10%	6%	28%	56%	91%	20%	74%
0.5 °C percentage error (%)	45%	50%	41%	72%	78%	96%	51%	89%

These evaluation criteria show that this calibration methodology can achieve highly precise results. The values in Table 23 above show smaller discrepancies between the measured and calibrated indoor temperature than what has been previously accepted in literature.

5.1.1.3. Calibration results for School 4

During the calibration procedure for this school, one of the indoor sensors encountered a malfunction, leading to the loss of a few days' worth of data points. In order to complete the calibration, a period of consecutive 3 weeks for the calibration and another 3 weeks that follow that period is required. This time frame ensures the attainment of accurate results, by assuming

there are minimal changes in human behavior within the three-week period. Furthermore, this time period provides a sufficient window for conducting an accurate investigation into the temperature fluctuations experienced by the school. Therefore, for the unoccupied period, R 215 was excluded from the calibration due to the missing data. However, it was included for the calibration period while the school was occupied for which it had a complete data set.

Table 24: Calibrated building parameters during the unoccupied period for School 4

Parameters	R 112	R 113	R 212	R 215
Shading solar reflectance	0.90	0.50	0.50	N/A
Air infiltration rate (ACH)	0.10			
Wall insulation U-value (W/m^2-K)	0.30			
Roof insulation U-value (W/m^2-K)	0.25			

Table 25: Evaluation criteria results during the unoccupied period for School 4

Evaluation criteria	Calibration				Validation			
	R 112	R 113	R 212	R 215	R 112	R 113	R 212	R 215
RMSE (ºC)	0.7	0.6	0.4	N/A	0.9	0.7	0.5	N/A
NMBE (%)	1.9	-1.2	-0.5	N/A	1.9	-0.6	-0.8	N/A
Max diff. (ºC)	2.0	1.4	1.5	N/A	2.0	1.5	1.6	N/A
1 °C percentage error (%)	19%	12%	1%	N/A	16%	13%	3%	N/A
0.5 °C percentage error (%)	54%	49%	19%	N/A	54%	42%	22%	N/A

Table 26: Calibrated building parameters during the occupied period for School 4

Parameters	R 112	R 113	R 212	R 215
Max NV amount (ACH)	5.00	5.00	6.00	6.00
NV setpoint (ºC)	21.00	21.00	22.00	22.00
Maximum lighting load (W/m^2)	9.00	9.00	9.00	9.00
Shading solar reflectance	0.65	0.15	0.50	0.60

Table 27: Evaluation criteria results during the occupied period for School 4

Evaluation criteria	Calibration			
	R 112	R 113	R 212	R 215
RMSE (ºC)	0.7	0.7	0.6	0.7
NMBE (%)	1.6	0.3	0.4	-0.8
Max diff. (ºC)	2.7	2.3	2.6	2.7
1 °C percentage error (%)	14%	17%	10%	14%
0.5 °C percentage error (%)	43%	47%	29%	50%

5.1.2. Summary of Findings for Calibration of Schools

After calibrating four schools to validate this calibration method, the following findings were also identified. Even though all the schools are based on the optimized solution calculated in jePlus, each school is fine-tuned in DesignBuilder. When using jePlus, the most difficult part was ensuring that all the input files were correctly submitted, and the parameters were given the correct intervals. Once this is set-up, the program can run through the python scripts and input files, which includes the base model from DesignBuilder and current weather data, in addition to parameter ranges, to produce a set of solutions to be used as the input parameter for DesignBuilder to calibrate the base model. This model can then be subjected to extra fine-tuning as described below.

First, it is very important to get the correct geometry before beginning the calibration process. With the use of Google Earth, it is possible to get an accurate reading of the degrees from the north to which the school is oriented. Next, having access to building plans is very helpful in tracing the correct dimensions, with the help of Google Maps if needed. Lastly, ensuring that the window-to-wall ratio accurately represents the real building can have a significant effect on building envelope calibration and consequently affect the overheating risk assessment. For example, it was found with School 3 that the small size of the windows is likely responsible for the low risk of overheating. Window size is important to accurately represent in the model, because it can affect many of the input parameters, such as solar heat gain coefficient, window U-value and natural ventilation due to its relation to window opening size. This leads to the next step of calibrating the building envelope, which needs to be properly calibrated before continuing to calibrate the occupancy loads. The wall and roof U-value and infiltration rate were often calibrated first to determine the overall daily temperature fluctuations of the model. Window U-value and SHGC are the next parameters to be calibrated and then finally the solar reflectance of shade rolls is often the last parameter to be calibrated. This is a general order and is not strictly linear, sometimes needing to go through several iteration processes. However, the solar reflectance of shade rolls which is the percentage of the window area that is covered by the shade roll. The higher the percentage, the more the window's shade has been pulled down. This part is all done in DesignBuilder starting with the whole building first and then it is continued at the room-level. Following this process, it is then repeated with the occupant-related building parameters. First, equipment density had little effect

on all schools. Next, natural ventilation was calculated using DesignBuilder's Fabrics and Ventilation function. To do this, the model's natural ventilation rate is set to be calculated (to be calculated by DesignBuilder), all the windows are closed, and infiltration rate is assumed to be virtually zero. The result of this simulation allows us to check the maximum ventilation at any given time during the year to create the range for this parameter. By setting the infiltration rate to virtually zero, the program is able to calculate the maximum natural ventilation rate that will be used as the natural ventilation rate for the school without taking into account the effect of building infiltration rate. However, the infiltration rate was already calculated in the first part of the calibration process (when the building was unoccupied), and so this simulation is only performed to check the maximum range of the building's infiltration rate, therefore once this test is performed, the infiltration rate is returned to the calibrated value from the first part of the calibration. Subsequently, lighting, occupancy, natural ventilation rate and setpoint are adjusted to achieve the final calibrated model.

Starting with natural ventilation, this building parameter had the greatest effect for all school buildings. The natural ventilation rate refers to the amount of air exchanges that is happening with window opening. Therefore, ensuring that the value for the free aperture for windows in the Openings tab in DesignBuilder was a significant input parameter. For some schools, the part of the window that was able to open was 33% and for others it was up to 50%. The scheduling of the natural ventilation was also important. It was often assumed that the windows were closed on weekends and holidays and when the school was not open. However, in certain situations, natural ventilation can be introduced during nighttime hours, resulting in a substantial reduction of simulated indoor building temperatures. If this improved the results, it can be assumed that there's a possibility that nighttime cooling is being used in this building or that a window was left open overnight by accident. On the other hand, natural ventilation should be removed or reduced during the daytime when the simulated daytime indoor temperatures are too low. When turned off during the day, this can either increase or decrease the simulated indoor temperature depending on whether the indoor temperature was hotter or colder than the outdoor air, the rate and the amount of time natural ventilation has time to affect the indoor temperatures. Opening a window can also offer a degree of cooling and cross-ventilation; however, it can trigger an increase in room temperature as hot air enters, but only when the outdoor temperature surpasses the indoor temperature. Thus, natural ventilation can effectively lower indoor temperature if the outdoor temperature is cooler.

Next, mechanical ventilation can also be modified similarly to the way natural ventilation is modified to change temperature fluctuations in a simulated building. Even though it may not provide cooling, which was the case for the schools included in this study, it acts very well for cooling down the building at night, and is more secure than natural ventilation, i.e. open windows at night can pose a safety hazard, while mechanical ventilation can be run all night without affecting the security of the building. Hence, it is crucial to contemplate augmenting mechanical ventilation rates during nighttime if there are observed reductions in indoor temperatures during that period.

Other building parameters that had a significant effect on the school's indoor temperature were lighting and occupancy. Increasing the lighting power density at night can increase the indoor temperature of the simulated building. It is possible that some lights are either left on at night for

safety reasons and/or by accident. Occupants will also increase indoor room temperatures. More occupants will increase internal loads. Therefore, removing them will decrease indoor air temperatures and adding them will increase indoor air temperatures. And, like all the other building parameters mentioned above, the schedules for these input parameters sometimes required special attention to correctly model the existing building's activities.

Lastly, some exceptional assumptions were made to account for COVID restrictions. All data discussed in this thesis was taken partially or fully under covid restrictions. While the exact measures cannot be identified, the following assumptions were thought to have had significant effects on the indoor temperature changes. For example, for School 1, the calibration was performed in a time period in May 2020, due to school closures at the time. However, in 2021, the school was reopened, and the unoccupied periods needed to be taken in July and/or August. In some cases, an elevated level of natural ventilation was presumed to be adopted by the schools, following COVID guidelines, which aimed to increase ventilation rates and mitigate the risks of air contamination by enhancing air exchange rates. In School 4, there were suspicions that one of the classrooms remained unused, possibly due to reduced class sizes, school closures, and/or the adoption of a hybrid model involving online learning. The models were adapted accordingly to account for these assumptions using special scheduling for specific rooms.

Table 28: Examples of solutions for calibration troubleshooting

Building Parameters	Indoor temperature is too high	Indoor temperature is too low
Natural Ventilation Rate	Increase, especially if outdoor air is cooler	Decrease, unless outdoor air is hotter
Mechanical Ventilation	Increase	Decrease
Lighting Power Density	Decrease	Increase
Occupancy Density	Decrease	Increase
Solar Reflectance of Shade Roll	Increase	Decrease

5.2. Calibration for Hospital Buildings

5.2.1. Calibration of Hospital 1

Hospital 1 was originally built in 1926. It features many different hospital wings for a variety of patients. Similarly, to the schools, the hospital features brick veneer walls, concrete roof, double-pane windows and approximately 30-40% window-to-wall ratio. While the entirety of the hospital appears to be modelled, only the block in grey (shown in Figure 16) was studied. This section of the building is a long-term care wing that is naturally ventilated. Indoor temperature data was collected from three rooms on the 5th floor of this block.

Figure 15: Snapshot taken from Google Earth of Hospital 1

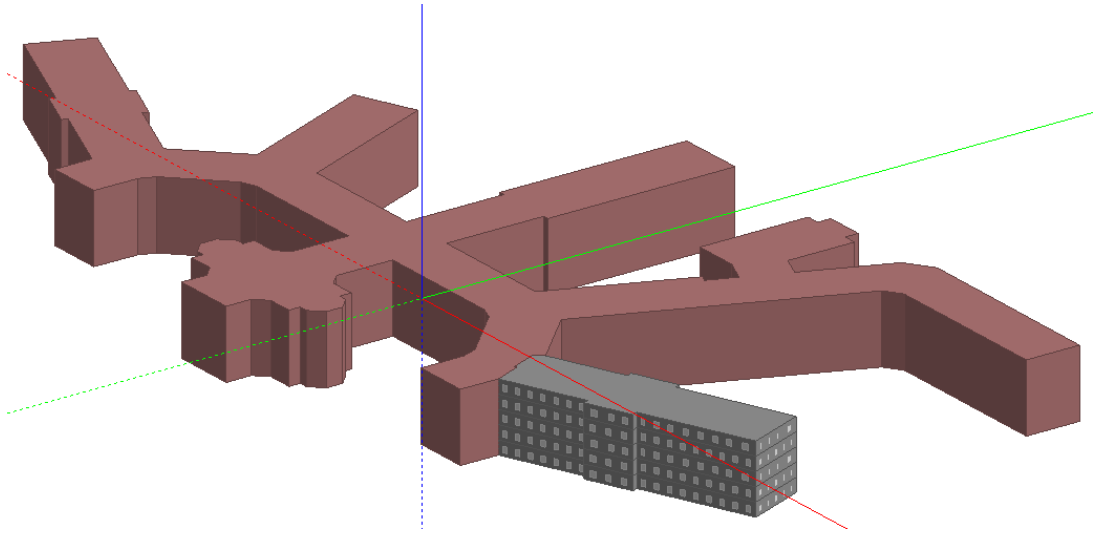

Figure 16: Snapshot of Hospital 1 modelled in DesignBuilder

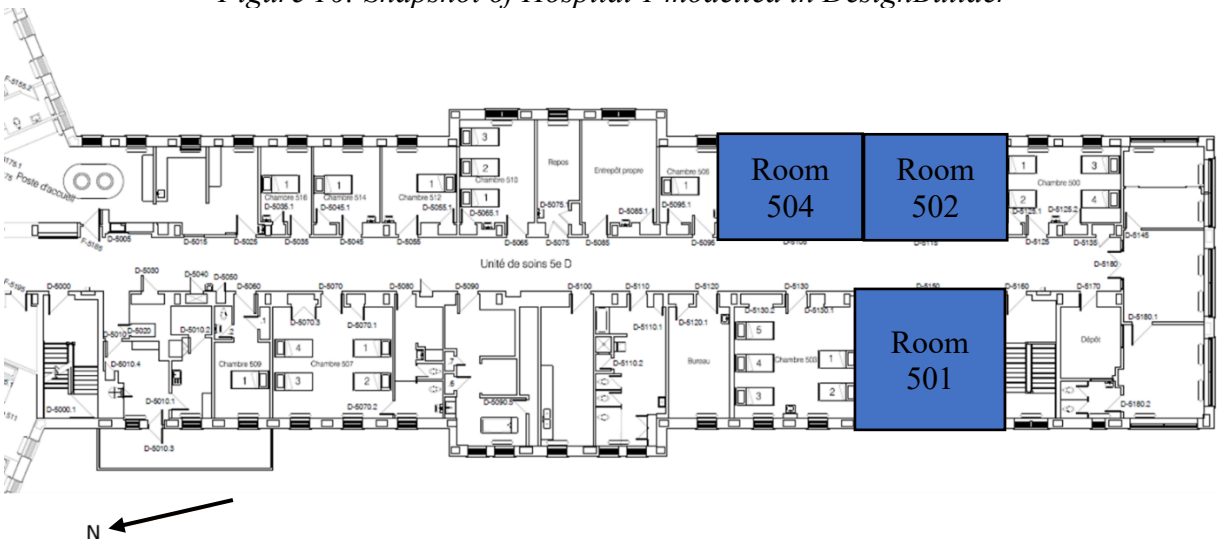

Figure 17: Building Plan of the location of the measured rooms in Hospital 1

5.2.1.2. Calibrated Parameters

Because the building is always occupied, unlike the school calibrations, all building envelope and occupancy related parameters were calibrated simultaneously. The calibration period for this building was from July 6, 2021 to July 27, 2021 and the validation period was from July 28, 2021 to August 17, 2021.

Table 29: Calibrated building parameters for all rooms unless otherwise specified for Hospital 1

Building Parameters	**Calibrated Value**
Max Air Infiltration Rate (ACH)	0.25
Wall U-value (W/m^2-K)	0.40
Roof U-value (W/m^2-K)	0.25
Window U-value (W/m^2-K)	2.60
Solar Heat Gain Coefficient	0.75
Solar Shade Reflectance	0.80 0.60 (Room 504)
Max Occupancy	1
Natural Ventilation Rate (ACH)	3
Natural Ventilation Setpoint (°C)	22
Lighting Power Density (W/m^2)	5
Equipment Power Density (W/m^2)	2

5.2.1.3. Performance Metrics

Table 30: Evaluation criteria results for Hospital 1

Measurement criteria	Room 501		Room 502		Room 504	
	Calibration	Validation	Calibration	Validation	Calibration	Validation
RMSE (ºC)	0.7	0.7	0.7	0.7	0.5	0.6
NMBE (%)	1.7	1.5	0.6	0.1	0.3	0.2
Max diff. (ºC)	1.8	2.7	2.2	1.9	1.5	1.6
1 °C percentage error (%)	15%	12%	11%	15%	6%	7%
0.5 °C percentage error (%)	44%	44%	48%	43%	31%	38%

With all RMSE values under 0.8°C and equal or less than 15% of the temperature differences between calibrated and simulated results being under 1°C for both the calibration and validation periods, this model shows a high level of accuracy using this calibration method.

5.2.2. Summary

While some of the same findings for the school calibrations apply to the hospital building, one of the major differences was the complexity of the hospital geometry. Choosing a large enough

section of the building without modeling the entirety of the building was important to reduce computing time. In this case, only one wing of the hospital was studied, with all three rooms situated on the same floor. The building's function as a long-term care wing was also a critical factor to consider. This meant that only one to two people per room would be permanently staying in that room, unless the room was unused. The building envelope of this hospital was also very similar to that of the one found for School 1, because they were built around the same time. All the other parameters are calibrated similarly to schools, but with less variation. It seems that hospital conditions are a lot more stable, which could be due to the low occupancy. With less people, there are less changes in human-behavior, creating a more constant environment day to day. This allowed for a quick calibration of this hospital, once its geometry was correctly set up, with no major issues arising.

5.3. Calibration for Residential Buildings

5.3.1. Calibration of a residence at Residential 1

This residential building was originally constructed in 1962 and featured yellow brick veneer wall. However, in 2018, Residential 1 underwent major renovations, with a new red brick veneer wall and new double-paned, low U-value windows. There are two measured apartments, one is located on the first floor with the temperature sensor placed in the bedroom and the other one is located on the third floor with the temperature sensor placed in the living room. The two pink blocks in Figure 18 (on the right) below represent nearby buildings.

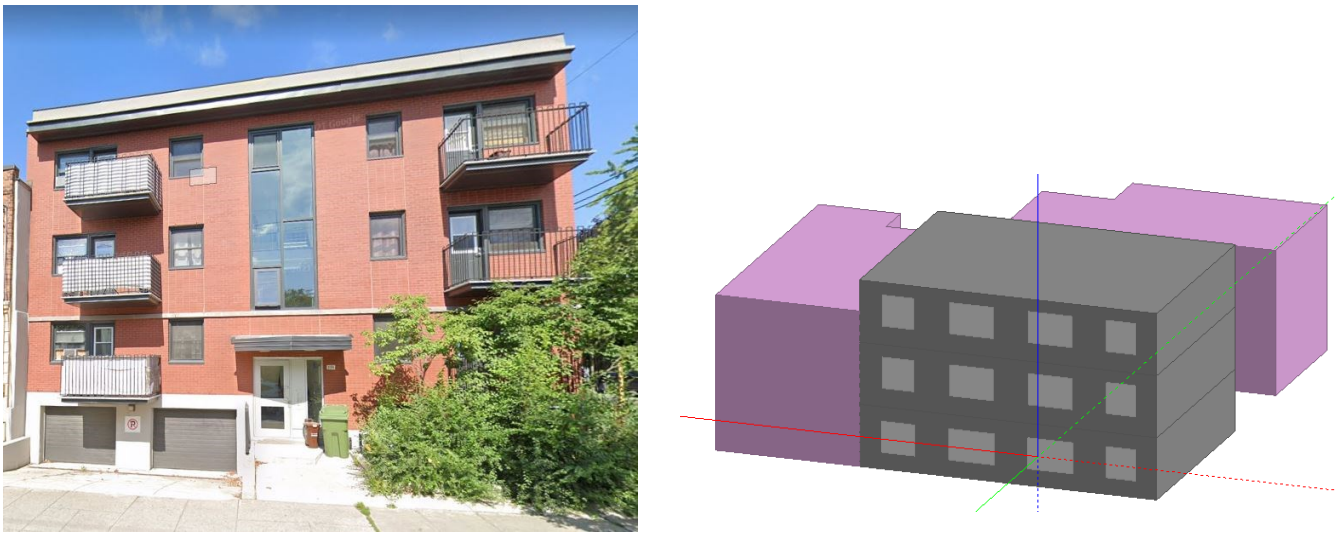

Figure 18: Google streetview of Residential 1 (left) and its axonometic view of its building model in DesignBuilder (right)

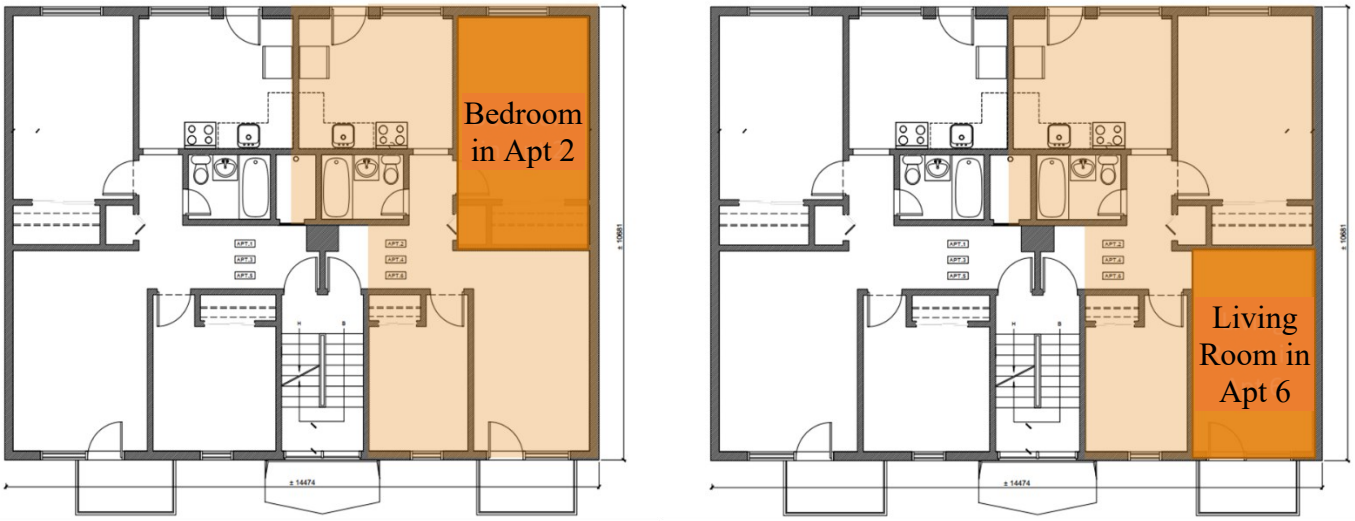

Figure 19: Plan views of the measured rooms in Residential 1

5.3.1.2. Calibrated Parameters

Similarly, to the hospital building, residential buildings are occupied all year round unlike the school buildings, so the calibration was completed in one phase while including all the building parameters and occupancy parameters. This building was calibrated from July 1, 2021 to July 22, 2021 and validated from July 23, 2021 to August 12, 2021. The resulting calibrated building parameters are shown in the table below. The types of schedules used for this building assumed that the occupants were out of the apartments during working hours (Monday to Friday, 9 to 5 pm) and were home all day on weekends.

Table 31: Calibrated Building Parameters for all rooms unless otherwise specified for Residential 1

Building Parameters	**Calibrated Value**
Max Air Infiltration Rate (ACH)	0.10
Wall U-value (W/m^2-K)	0.16
Roof U-value (W/m^2-K)	0.12
Window U-value (W/m^2-K)	0.80
Solar Heat Gain Coefficient	0.45
Solar Shade Reflectance	0.60 (Apt 2) 0.30 (Apt 6)
Max Occupancy	5
Natural Ventilation Rate (ACH)	5
Natural Ventilation Setpoint (°C)	24
Lighting Power Density (W/m^2)	5
Equipment Power Density (W/m^2)	2

5.3.1.3. Performance Metrics

It is notable that this building had some of the best results according to the evaluation criteria. It is also the most recently renovated building, where its building envelope was significantly improved. All the RMSE values are equal to or less than 0.7°C and most of the NMBE values are close to zero. The maximum differences are on the higher side, but remain under 3°C. And finally, the percentage of calibration results having less than 1°C difference between measured and simulated stays under 15% and under 50% for those less than 0.5°C difference. Calibrating only two rooms also reduced the amount of time required to achieve a fully calibrated model. It is also a smaller building, with only 6 apartments total, 2 per floor with a total of 3 floors. The neighbouring buildings were also modeled as adjacent buildings with adiabatic surfaces in between the separate buildings. This type of building type in DesignBuilder allows for heat transfer between buildings, assuming all buildings have similar insulation and indoor temperature, without requiring a full simulation of the adjacent buildings. It was necessary to add these component blocks, because they were in close proximity to the residential building and might have a small effect in terms of shading and/or heat absorption.

Table 32: Evaluation criteria results of measured rooms for Residential 1

Measurement criteria	Apt 2		Apt 6	
	Calibration	Validation	Calibration	Validation
RMSE (ºC)	0.6	0.7	0.7	0.7
NMBE (%)	-0.03	1.4	-0.1	0.2
Max diff. (ºC)	2.6	2.5	2.2	2.2
1 °C percentage error (%)	11%	14%	13%	20%
0.5 °C percentage error (%)	38%	38%	49%	49%

5.3.2. Summary

Similarly, to hospitals, the building envelope was quick to calibrate. In this case, the building envelope was recently renovated, so it was well within the reasonable range for current building standards. Detailed building plans were also provided, therefore creating the building geometry and orientation was easy to recreate with high accuracy. And so, the combination of good building geometry and orientation and a well-insulated building envelope allowed for the building envelope to be quickly calibrated. The natural ventilation and solar reflectance of shade rolls were the most difficult part of the calibration. For residential buildings, the location of windows was important for security and privacy concerns. Human influence, likely driven by privacy and security concerns, directly impacted the window shading preference, resulting in a solar shade reflectance of 60% for the first-floor apartment and 30% for the top-floor apartment. The natural ventilation setpoint was also set to 24°C which is a bit high, but from the installation notes, it was mentioned that the family that had moved into the top apartment was used to a hotter climate.

6. Assessment and Mitigation of Overheating Risks

Following the calibration of the buildings in this study, these calibrated models were used to calculate the number of overheating hours to assess and mitigate the risk of overheating. Two different sets of criteria were used to assess the overheating risks amongst the three types of buildings. CIBSE TM52 criteria were used to assess School 3 and School 4 with school-aged children of 5 to 12 years old. This system is tailored for school children, using Category 1 for sensitive and/or vulnerable patrons, under which young children fall. ASHRAE 55 was used for Hospital 1 and Residential 1. The hospital assessment and residential building assessement followed the 40-hour limit for vulnerable patrons (young, elderly and/or sick).This assessment is conducted using 2020, 2044 and 2090 weather data, which were the years determined by Baba et al. to be the most intense and severe in the short-, mid- and long-term years (Baba et al., 2023).

For the school models, overheating hours were calculated based on CIBSE TM52 as mentioned in Chapter 2. CIBSE TM52 is an input parameter that is included in DesignBuilder and is able to calculate the percentage of overheating hours during the summer season as per its criteria by including it as an input parameter before running the simulation over one whole year. Once the simulation is complete, the values calculated according to CIBSE TM52 by DesignBuilder are then exported to Excel and the zones that have overheating hours within the acceptable range as determined by CIBSE TM52 to present a value that is less than 4.5% of the total summerttime hours. This process is then repeated with future climate data and then again with mitigation techniques to determine which techniques can have the greatest impact in the current and future climate.

This process is then repeated with the hospital and residential building, however the thermal comfort criteria used for these buildings come from ASHRAE 55's 80% acceptability level, where a maximum of 200 overheating hours is allowed for healthy patrons and a maximum of 40 overheating hours is allowed for vulnerable patrons, such as young children, elderly people and/or people who are ill. This system is also integrated in the DesignBuilder software. The program is able to calculate the number of overheating hours over the year and this information is exported into an Excel worksheet where zones that surpass the number of overheating hours according to the acceptability limits are identified and are at risk of overheating.

Once the buildings are assessed for overheating risks, various mitigation strategies are applied individually and/or in combination. Mitigation techniques that are applied include a 1.5 m overhang, a pair of 1.5 m sidefins, exterior shade roll, cool roofs and/or walls with an absorptivity of 20%, green walls and/or roofs, and night cooling. These strategies were selected based on the existing literature that proved to be effective in mitigating overheating risks (Baba, 2022). The addition of overhangs, sidefins and exterior shade rolls are mitigation strategies that make use of exterior shading to prevent heat from entering the building from the outside. Overhangs are horizontal shades that are installed at the top edge of windows. Sidefins are vertical shades that are installed on both sides of each window. Cool roofs and walls have a higher albedo, which provides a more reflective surface so that the building does not absorb as much heat as a conventional rooftop. On the other hand, green roofs and walls have the ability to absorb sunlight through its plantation to reduce the amount of heat transfer to the building. Finally, night cooling takes advantage of the cooler nighttime temperatures by leaving windows open at night to enable

natural ventilation. With the colder outdoor temperature, cooler air can enter the building from the bottom floor windows and push hotter air up and out of the upper floor windows. This enables the building to cool off at night and prevent heat from carrying over into the next day. If a singular technique is not enough to mitigate the overheating risks in all zones of the buildings, then techniques are combined to find a solution that works. Some combinations include overhangs with cool roofs, exterior shade roll with night cooling, etc.

6.1. School Buildings

The evaluation of classrooms was performed according to BB101 which follows CIBSE TM52 requiring overheating hours to be less than or equal to 4.5% total hours over the summer period only (May to August), Monday to Friday, from 9 am to 4 pm. Classrooms that exceed this percentage are indicated in red in Table 33 to 37.

6.1.2. Overheating and Mitigation for School 3

School 3 does not appear to experience any major overheating issues in the current climate, except for the one classroom (Zone 26). As explained earlier, this is the case because this room has a different function than the rest of the classrooms in this building, has much larger windows than any of the other classrooms and appears to be built from different materials. As shown in Table 33, only zone 26, experiences overheating in 2020 and continues to have the highest overheating risk in future years as shown in red below, while the other rooms remain below the acceptability limit as shown in green. By 2044, most of the rooms remain under 10%, which is more than double the acceptability rate, with 10 rooms reaching up to close to 40%. And finally, by 2090, most rooms will reach close to 20%, doubling the amount of summertime overheating hours again. Therefore, while this school did not experience major overheating in 2020, it will require some building modifications to ensure it does not overheat in the future.

Table 34, 35 and 36 present the mitigation strategies applied, where the first column shows the zone being evaluated and the second column shows the percentage of overheating hours without mitigation measures applied for reference. Starting with the year 2020, using DesignBuilder, window overhangs projecting by 1.5 m were added above each window to reduce the amount of overheating. While this measure had a great effect on zone 26, the amount of overheating was still not reduced to below the acceptability limits. Thus, the next mitigation strategy used was the use of a cool roof. This cool roof had a solar absorptance of 20%, as compared to a conventional roof with 85%, which increased the albedo of the roof. This should have a great impact on all rooms, because the building is only one storey high. While it did have a positive effect on all rooms, it only reduced the percentage of summertime overheating of zone 26 by approximately 30%. Lastly, the rolling blind shades were switched to be installed on the outside of the building, which finally reduced the overheating risk in zone 26 to zero. From this calculation, a conclusion was drawn that this school's overheating risk was considerably low, due to its small windows. While the exterior shade rolls had a major effect on the classrooms with very large windows, it had a smaller effect on the classrooms with smaller windows.

Table 33: Percentage of overheating hours over the summer period by zone for School 3

	2020	2044	2090
Zone 01	0.13	8.04	19.16
Zone 02	0.09	7.67	15.94
Zone 03	0.1	9.1	16.81
Zone 04	0.12	7.32	15.95
Zone 05	0.13	6.85	15.67
Zone 06	0.13	6.83	15.7
Zone 07	0.12	6.64	15.33
Zone 08	0.16	17.87	22.5
Zone 09	0.12	6.23	15.19
Zone 10	0.15	7.1	16.84
Zone 12	0.13	6.57	14.65
Zone 13	0.12	9.64	19.65
Zone 15	0.15	6.9	16.86
Zone 16	0.15	9.12	17.17
Zone 19	0.25	36.35	31.71
Zone 20	0.21	21.75	26.07
Zone 21	0.98	25.04	33.49
Zone 24	0.16	8.63	19.47
Zone 25	0.1	12.5	19.05
Zone 26	21.57	37.53	37.96
Zone 28	0.1	18.14	23.29
Zone 29	0.13	3.59	10.77
Zone 30	0	9.51	16.33
Zone 32	0.85	15.68	24.13
Zone 33	0.15	12.58	21.27
Zone 35	0.12	3.68	11.63
Zone 36	2.06	15.54	27.93
Zone 37	0.12	7.94	17.47
Zone 38	0.15	6.55	16.19

Table 34: Overheating and individual mitigation measure applied to School 3 in 2020

2020	Overheating (%)	Overhang (%)	Cool Roof (%)	Exterior Shade Rolls (%)
Zone 01	0.13	0.13	0	0.13
Zone 02	0.09	0.07	0	0.04
Zone 03	0.1	0.09	0	0.06
Zone 04	0.12	0.12	0	0.12
Zone 05	0.13	0.12	0	0.12
Zone 06	0.13	0.12	0	0.12
Zone 07	0.12	0.12	0	0.1
Zone 08	0.16	0.13	0.1	0.12
Zone 09	0.12	0.1	0	0.1
Zone 10	0.15	0.15	0.01	0.13
Zone 12	0.13	0.12	0	0.12
Zone 13	0.12	0.1	0	0.09
Zone 15	0.15	0.13	0.03	0.13
Zone 16	0.15	0.13	0.09	0.12
Zone 19	0.25	0.16	0.13	0.12
Zone 20	0.21	0.13	0.09	0.12
Zone 21	0.98	0.19	0.13	0.13
Zone 24	0.16	0.15	0.04	0.13
Zone 25	0.1	0.03	0	0
Zone 26	21.57	6.37	14.62	0
Zone 28	0.1	0	0	0
Zone 29	0.13	0.12	0.03	0.12
Zone 30	0	0	0	0
Zone 32	0.85	0	0	0
Zone 33	0.15	0.13	0.1	0.12
Zone 35	0.12	0.1	0	0.1
Zone 36	2.06	0.22	0.21	0.12
Zone 37	0.12	0.12	0	0.1
Zone 38	0.15	0.13	0.01	0.13

The above process for finding a mitigation strategy that worked to reduce the overheating hours below the acceptability level was repeated for 2044 and 2090, as shown in the Tables 35 and 36, respectively. However, in 2044, the mitigation strategy required more than the use of exterior shade rolls. It was found that a combination of exterior shade rolls, and the use of a cool roof was required to reduce the amount of overheating below the 4.5% threshold. And so, in terms of applicability of major renovations to mitigation current and future overheating, the use of exterior shade rolls should be installed as soon as possible, while the cool roof must be installed before 2044.

Table 35: Overheating and mitigation measures applied to School 3 in 2044

2044	Overheating (%)	Overhang (%)	Cool Roof (%)	Exterior Shade Rolls (%)	Cool Roof + Overhang (%)	Cool Roof + Ext Shade Roll (%)
Zone 01	8.04	5.58	0.56	3.75	0.2	0.13
Zone 02	7.67	6.57	0.7	3.82	0.43	0.13
Zone 03	9.1	7.86	1.3	5.15	1	0.32
Zone 04	7.32	6.06	0.6	3.54	0.34	0.07
Zone 05	6.85	5.49	0.43	3.24	0.25	0.04
Zone 06	6.83	5.47	0.42	3.25	0.25	0.04
Zone 07	6.64	5.49	0.39	3.27	0.31	0.04
Zone 08	17.87	8.7	6.41	2.95	0.9	0.03
Zone 09	6.23	4.56	0.48	2.31	0.17	0
Zone 10	7.1	5.72	0.58	3.48	0.24	0.07
Zone 12	6.57	4.52	0.41	2.34	0.13	0
Zone 13	9.64	7.04	1.78	4.91	0.86	0.22
Zone 15	6.9	5.27	0.55	3.66	0.25	0.08
Zone 16	9.12	4.38	1.21	2.3	0.18	0
Zone 19	36.35	29.26	24.13	4.71	12.53	0.32
Zone 20	21.75	14.56	7.77	5.65	3.21	0.35
Zone 21	25.04	12.57	11.34	4.63	3.87	0.38
Zone 24	8.63	6.33	1.35	4.73	0.53	0.21
Zone 25	12.5	5.81	1.77	2.72	0.18	0.04
Zone 26	37.96	22.71	30.67	0.31	20.76	0.08
Zone 28	18.14	6.93	5.89	3.07	0.66	0.07
Zone 29	3.59	1.49	0.06	0.55	0	0
Zone 30	9.51	1.36	2.4	0.04	0.56	0
Zone 32	15.68	3.49	6.44	0.17	1.42	0
Zone 33	12.58	10.49	3.73	1.89	2.41	0
Zone 35	3.68	3.11	0.04	1.43	0	0
Zone 36	15.54	10.54	5.98	2.58	2.79	0.03
Zone 37	7.94	6.24	0.83	3.25	0.31	0.06
Zone 38	6.55	5.11	0.52	2.65	0.21	0.01

Based on the findings from 2044, employing exterior shade rolls and cool roof is deemed suitable for 93% of the rooms, including Zone 26, and will be used as a foundation for future development in 2090.The two rooms that will experience overheating in 2090, using the mitigation solution from 2044, are close to the threshold, but surpass it by less than 15%. Zones 20 and 21, which are classrooms that are adjacent to each other also experience more overheating than the other rooms due to their position. Zone 20 is one of the smallest classrooms with two small windows and Zone

21 is south facing with two openings that are south facing: one window and a set of double doors. Therefore, these two classrooms will receive the most direct sunlight during the summer, which explains the amount of overheating they experience. And so, the additional use of overhangs by 2090 is required to eliminate the risk of overheating for all rooms.

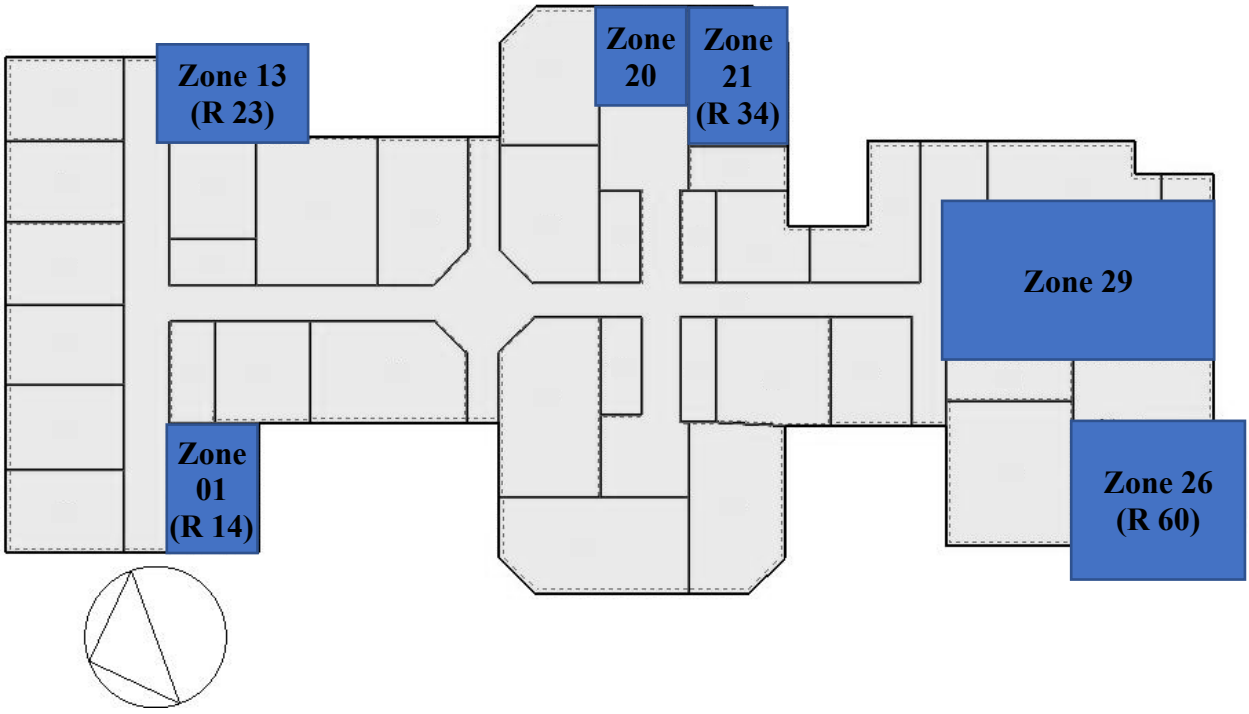

Figure 20: Plan view of School 3

Table 36: Percentage of overheating hours when mitigation measures are applied to School 3 in 2090

2090	Overheating (%)	Cool Roof + Ext Shade Roll (%)	Cool Roof + Overhang + Ext Roll (%)
Zone 01	19.16	3.47	3.32
Zone 10	16.84	2.99	2.86
Zone 12	14.65	2.3	2.15
Zone 13	19.65	4.28	3.87
Zone 15	16.86	2.96	2.81
Zone 16	17.17	2.38	2.15
Zone 19	31.71	3.97	3.52
Zone 02	15.94	3.56	3.47
Zone 20	26.07	4.64	3.93
Zone 21	33.49	5.16	4.29
Zone 24	19.47	4.01	3.55
Zone 25	19.05	2.44	2.24
Zone 26	37.53	2.44	1.75
Zone 28	23.29	2.95	2.22
Zone 29	10.77	1.59	1.15
Zone 03	16.81	3.97	3.82
Zone 30	16.33	1.11	0.88
Zone 32	24.13	1.49	0.91
Zone 33	21.27	2.64	2.38
Zone 35	11.63	1.71	1.57
Zone 36	27.93	3.76	2.99
Zone 37	17.47	2.86	2.68
Zone 38	16.19	2.67	2.55
Zone 04	15.95	3.04	2.95
Zone 05	15.67	2.85	2.69
Zone 06	15.7	2.82	2.71
Zone 07	15.33	2.92	2.83
Zone 08	22.5	2.61	2.29
Zone 09	15.19	2.33	2.2

Overall, the risk of overheating at School 3 can be considered minimal and is potentially this way due to the small window-to-wall ratio of this building, and the lack of many south-facing windows. The addition of a cool roof would also be a great solution for this one-storey building, as it will be able to directly affect all classrooms. And finally, the mitigation solution for this building can be applied in steps, by first adding exterior shade rolls, then installing a cool roof and then window overhangs, to mitigate all overheating risk by 2090.

6.1.2. Overheating and Mitigation of School 4

School 4 appears to have more overheating issues for the majority of the building in the current and future climate than School 3. As shown in the table below, all zones will experience an excessive number of overheating hours in 2020, 2044 and 2090. The zone with the highest percentage of overheating hours per year is indicated in red, which is room 212, located on the second floor of the original building, for all three years.

Table 37: Percentage of overheating hours over the summer period by zone at School 4

Block	Zone	2020	2044	2090
Block1	112	15.63	37.75	41.43
Block1	113	23.11	51.37	56.1
Block2	212	40.94	68.83	77.67
Block2	215	25.25	64.82	72.59
Block2	Zone 05	38.53	66.54	74.78
Block2	Zone 06	39.29	67.14	75.98
Block2	Zone 07	36.56	64.98	72.12
Block2	Zone 09	39.57	67.09	76.25
Block2	Zone 13	37.55	66.3	73.47
Block2	Zone 15	39.75	67.4	76.42
Block2	Zone 16	38.28	67.4	74.37
Block2	Zone 17	38.38	67.3	74.67
Block2	Zone 18	38.71	66.36	75.86
Block2	Zone 19	39.91	67.92	76.67

Compared to School 3, School 4 has a higher window-to-wall ratio and has two floors. It also has a large gymnasium and library and was built in phases. As mentioned in Chapter 2, it is possible that as buildings attempt to become more energy efficient, buildings may experience more overheating during the summertime. The rooms in Block 1 were part of the school extension in 1990, while the rest of the school was built in 1953. And, as shown in the tables below, one mitigation measure is not enough to reduce overheating hours to below the thermal comfort threshold for all extreme years. Already in 2020, exterior shade rolls and a cool roof are required to ensure that all zones are below the 4.5% acceptability limit. Zones below this limit are shown in green. However, by 2044, this solution is no longer acceptable. However, the use of exterior shade rolls in combination with night cooling does mitigate the overheating risk and continues to work for most rooms by 2090. Only three rooms experience too much overheating, which can be fixed with the addition of a cool roof. Therefore, for this school, the addition of exterior roll shades is needed for all three extreme years. And then, the use of night cooling, especially in the second-floor rooms, for security reasons, would also be effective for all three years and could be applied immediately. Night cooling is a great minimally obstructive strategy because it consists of a behavioral or system change without the installation of new, potentially costly equipment. And although night cooling was not tested as a solution in 2020, if this measure works in 2044, there is a high chance this measure is also effective in eliminating overheating in 2020. And so, night

cooling should be introduced immediately, if it is safe to do so, followed by the installation of exterior shade rolls and the eventual upgrade of the roof to a cool roof to mitigate overheating by 2090.

Table 38: Mitigation measures applied to School 4 in 2020

2020		Overheating (%)	Ext. Shade Roll (%)	Overhang (%)	Cool Roof (%)	Cool Roof + Ext. Shade Roll (%)
Block1	112	15.63	0.52	5.26	14.05	0.51
Block1	113	23.11	0.24	9.09	15.51	0.24
Block2	212	40.94	6.36	21.29	31.6	0.1
Block2	215	25.25	1.86	4.71	13.4	0.24
Block2	Zone 05	38.53	3.65	16.33	27.18	0
Block2	Zone 06	39.29	5.23	19.88	29.13	0
Block2	Zone 07	36.56	5.26	13.99	25.03	0.03
Block2	Zone 09	39.57	4.87	19.7	28.06	0
Block2	Zone 13	37.55	5.32	16.1	26.4	0.03
Block2	Zone 15	39.75	5.14	19.95	28.33	0
Block2	Zone 16	38.28	5.42	16.59	27.18	0.04
Block2	Zone 17	38.38	4.53	17.54	27.96	0
Block2	Zone 18	38.71	4.43	19.09	27.15	0
Block2	Zone 19	39.91	5.66	20.23	29.03	0.07

Table 39: Mitigation measures applied to School 4 in 2044

2044		Overheating (%)	Cool Roof + Ext Roll (%)	Ext Roll + Night Cooling (%)
Block1	112	37.75	12.71	0.14
Block1	113	51.37	7.55	1.89
Block2	212	68.83	21.58	0.56
Block2	215	64.82	15.08	1.12
Block2	Zone 05	66.54	23.3	0.81
Block2	Zone 06	67.14	21.03	0.52
Block2	Zone 07	64.98	21.9	0.72
Block2	Zone 09	67.09	20.61	0.49
Block2	Zone 13	66.3	22.12	0.73
Block2	Zone 15	67.4	20.69	0.52
Block2	Zone 16	67.4	23.55	0.74
Block2	Zone 17	67.3	24.45	0.81
Block2	Zone 18	66.36	20.65	0.49
Block2	Zone 19	67.92	21.21	0.53

Table 40: Percentage of overheating hours with mitigation measures applied to School 4 in 2090

2090		Overheating (%)	Ext. Shade Roll + Night Cooling (%)	Ext. Shade Roll + Cool Roof + Night Cooling (%)
Block1	112	41.43	1.77	1.37
Block1	113	56.1	6.83	3.69
Block2	212	77.67	3.66	1.53
Block2	215	72.59	4.58	2.53
Block2	Zone 05	74.78	4.09	1.73
Block2	Zone 06	75.98	3.48	1.5
Block2	Zone 07	72.12	3.43	1.45
Block2	Zone 09	76.25	3.53	1.45
Block2	Zone 13	73.47	3.68	1.58
Block2	Zone 15	76.42	3.54	1.45
Block2	Zone 16	74.37	3.69	1.55
Block2	Zone 17	74.67	3.76	1.59
Block2	Zone 18	75.86	3.37	1.28
Block2	Zone 19	76.67	3.51	1.47

In this case, there is no one mitigation strategy that is able to resolve overheating in all rooms. Therefore, a combination of mitigation measures is necessary to achieve comfortable indoor temperatures to meet the criteria set by CIBSE TM52 for Category 1 (sensitive) patrons. In 2020, the use of exterior shade rolls and either night cooling or cool roof will solve the overheating risk. In 2044, exterior shade rolls in combination with night cooling will be required to have all zones below the thermal comfort. In 2090, an exterior shade roll in combination with night cooling and cool roof will be necessary to avoid overheating. These strategies can be installed in phases as mentioned earlier to adapt the building as needed for all extreme years.

6.2. Hospital Buildings

As mentioned at the beginning of this chapter, the next two sections for hospital and residential buildings use ASHRAE 55's 80% Acceptability Limit for the thermal comfort threshold. This threshold was also adapted by the BC Energy Step Code that limits overheating hours to a maximum of 200 hours for healthy patrons and 20 hours for vulnerable patrons (Baba et al., 2023). Zones that exceed these numbers are at risk of overheating. For hospitals, it is especially important to respect the 20-hour limit, seeing as most patients will fall under the vulnerable patrons' description (Baba et al., 2023).

In Figure 21 below, it is shown that all measured rooms are overheated in all extreme years according to the above-mentioned thermal comfort threshold.

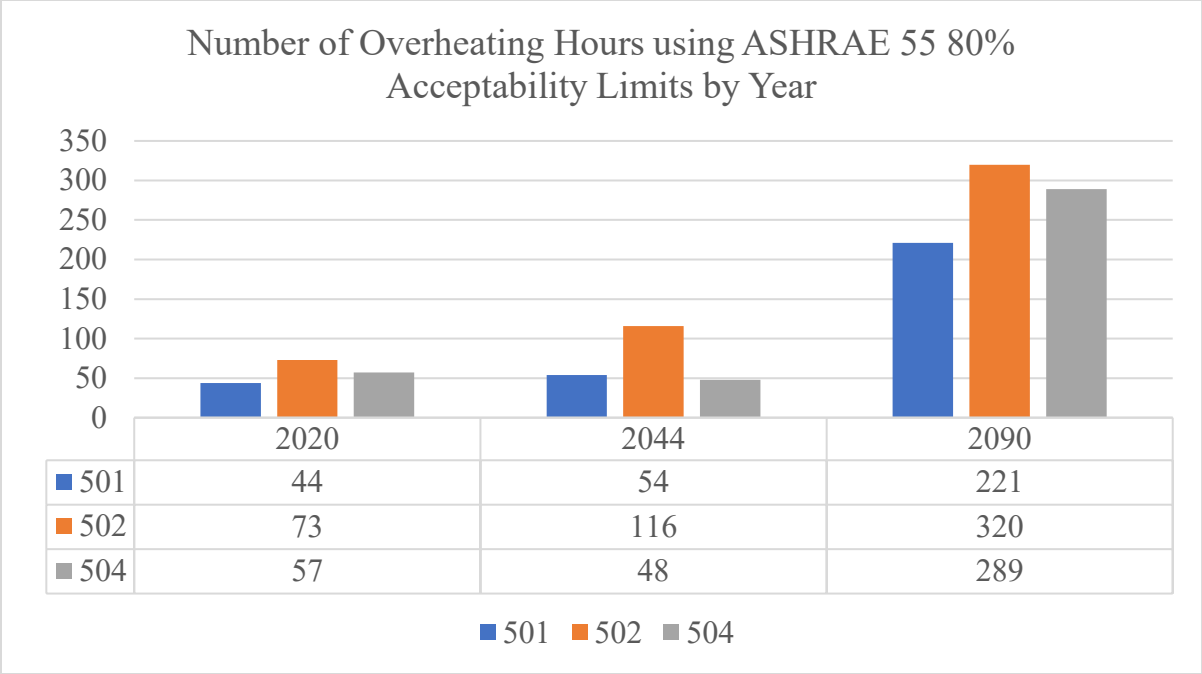

Figure 21: Number of Overheating Hours in Hospital 1

Therefore, mitigation techniques must be applied to assess what building modifications can be made to bring these overheating numbers below the thermal comfort threshold level. The results of these simulations are shown in the following table below. The numbers in red show the solutions that are not acceptable. In the year 2020 and 2044, exterior shading can resolve the overheating risk of this building. However, for the year 2090, exterior shade rolls in combination with cool walls are required to ensure thermal comfort for all patrons.

Table 41: Number of Overheating Hours using Various Mitigation Techniques and Combinations for Hospital 1

Year	Room	Overhang (hrs)	Sidefins (hrs)	Exterior Shade Roll (hrs)	Cool Wall (hrs)	Green Wall (hrs)	Cool Wall & Sidefin (hrs)	Cool Wall & Exterior Shade Roll (hrs)
2020	R 501	11	2	0	16	25	0	0
	R 502	18	3	0	3	5	0	0
	R 504	6	3	0	0	3	0	0
2044	R 501	33	10	0	28	65	0	0
	R 502	18	14	0	4	100	0	0
	R 504	15	11	0	2	34	0	0
2090	R 501	132	98	35	136	153	57	17
	R 502	153	135	44	137	151	55	19
	R 504	127	121	41	118	124	53	17

The overheating risk assessment for this hospital only covers the three rooms that had indoor sensors where data was collected. When the buildings were selected for this study, indoor sensors were installed in the most problematic rooms, i.e. the rooms that were experiencing the greatest amount of overheating as per the surveys. Therefore, it is assumed that one of these three rooms will most likely experience the greatest amount of overheating for this building. From the table above, room 502 had the highest risk of overheating, and that all three rooms will experience great amounts of overheating in 2090. Although exterior shade rolls and sidefins independently proved effective in reducing overheating to below 20 hours in 2020 and 2044, a combination of exterior shade rolls and cool walls will be necessary for 2090. Therefore, it is advisable to install exterior shade rolls in the near future and to later upgrade the walls to use high albedo wall material or to install sidefins and later exchange them for exterior shade rolls and cool walls by 2090.

6.3. Residential Buildings

Similar to hospitals, residential buildings follow ASHRAE 55, but can also follow CIBSE TM59 which is similar to CIBSE TM52 that was used for schools but is adapted for residential buildings. The acceptability limits for overheating hours remain at 200 hours for healthy patrons but is 40 hours for vulnerable patrons (Baba et al., 2023). In this building, the overheating in 2020 is considerably moderate, being under the 200-hour limit, but over the 40-hour limit in some zones and becomes increasingly problematic in the years 2044 and 2090 as shown in the table below. Yellow indicates rooms that fall below the 200-hour limit and green indicates the rooms that fall under the 40-hour limit.

Table 42: Overheating Hours for Residential 1

		Orientation	2020	2044	2090
First Floor - Apartment 2					
	Bedroom 2-1	North	0	0	54
	Bedroom 2-2	Southeast	75	453	492
	Living Room 2-1	Southeast	40	856	945
Third Floor - Apartment 6					
	Bedroom 6-1	North	86	101	304
	Bedroom 6-2	Southeast	136	586	662
	Living Room 6-1	Southeast	31	741	886

To mitigate these overheating hours, mitigation measures are necessary to reduce these numbers. In the table below, for apartment 2, it is shown that the use of exterior shade rolls reduces the number of overheating hours to below the limit of acceptability. However, for the other two extreme years, a combination of mitigation measures is required. For 2044, the use of a cool walls and exterior shade rolls in combination will reduce the number of overheating hours to zero. And, for 2090, the solution for 2044 plus the use of cool roofs will reduce the number of overheating hours to below 25 hours. The case is similar for apartment 6, however there is no solution to

mitigate overheating to below 20 hours in 2090. The suggested mitigation solution for this building is to install exterior shade rolls for the near and mid-future and later to change the roof and wall surfaces to use high albedo material to reduce overheating as much as possible by 2090. Night cooling may be an option to explore, as shown with the school buildings, however it is not ideal for residential buildings, due to noise pollution, air pollution and security reasons.

Table 43: Number of Overheating Hours using Various Mitigation Techniques and Combinations in Apartment 2

Zone	Overhang (hrs)	Sidefins (hrs)	Exterior Shade Roll (hrs)	Cool Wall (hrs)	Green Wall (hrs)	Cool Wall & Ext. Shade Roll (hrs)	Cool Wall + Roof & Ext. Shade Roll (hrs)
Year 2020							
Bedroom 2-1	0	0	0	0	0	0	--
Bedroom 2-2	37	42	6	51	73	1	--
Living Room 2-1	1	7	0	3	36	0	--
Year 2044							
Bedroom 2-1	0	0	0	0	0	0	--
Bedroom 2-2	166	137	0	355	430	0	--
Living Room 2-1	563	443	4	600	937	0	--
Year 2090							
Bedroom 2-1	24	34	0	34	27	--	0
Bedroom 2-2	274	301	66	393	380	--	24
Living Room 2-1	617	685	138	693	655	--	16

Table 44: Number of Overheating Hours using Various Mitigation Techniques and Combinations in Apartment 6

Zone	Overhang (hrs)	Sidefins (hrs)	Exterior Shade Roll (hrs)	Cool Wall (hrs)	Green Wall (hrs)	Cool Wall & Ext. Shade Roll (hrs)	Cool Wall + Roof & Ext. Shade Roll (hrs)
Year 2020							
Bedroom 6-1	46	59	0	64	87	0	--
Bedroom 6-2	84	107	23	116	131	8	--
Living Room 6-1	4	10	0	3	32	0	--
Year 2044							
Bedroom 6-1	77	81	0	79	116	0	--
Bedroom 6-2	339	291	13	450	556	1	--

Living Room 6-1	484	379	70	433	733	0	--
Year 2090							
Bedroom 6-1	214	245	67	247	242	--	6
Bedroom 6-2	510	527	219	595	586	--	78
Living Room 6-1	745	771	441	746	734	--	57

6.4. Summary

Throughout this process of assessing overheating risks among different types of buildings using both CIBSE TM52 for schools and ASHRAE 55 for hospitals and residential buildings, the following conclusions can be drawn: building orientation has a great effect on the amount of overheating that rooms may experience; external shading can be very effective in reducing overheating in buildings; the school buildings responded well to many types of mitigation strategies; the residential building experienced more overheating than expected despite having been recently renovated; mitigation solutions for four buildings were found; and the process for finding mitigation strategies was refined.

First, with building orientation, the rooms with windows that had the most exposure to the south and direct sunlight will cause those rooms to experience the most overheating, as shown with Room 23 in School 3 and Room 502 in Hospital 1. In these cases, overhangs were effective in mitigating this overheating risk. Conversely, rooms that were facing east or west would require sidefins. However, of all external shading, the exterior shade rolls were the most effective for all buildings out of the three types of external shading applied in this study, because it worked for all room orientations. And these external shading devices were shown to effectively block direct sunlight and heat from entering the building.

Next, it is worth noting that the overheating risk was seemingly easier to mitigate in schools than in the hospital and residential building. The difference between these two types of buildings is that the schools are only occupied during the daytime and are unoccupied at nighttime, while the hospital rooms and residential rooms are either occupied all day or have people sleeping in them at night. While schools and hospitals might be able to open the windows during the day when it gets too hot and/or adjust the shade rolls, houses that are unoccupied during the hottest time of the day are unable to be adjusted. And then, when the occupants come home at night to sleep, it is not always possible to use night cooling as a solution due to exterior noise and security concerns. Therefore, hospitals and residential buildings are restricted to using highly reflective surfaces, and/or to closing the shades before leaving the house to mitigate some overheating. It is also unexpected that the residential building performed relatively poorly for having been renovated in 2018, experiencing similar overheating to the hospital which was initially built in the mid-1900s. Thus, it can be concluded that newer construction is not necessarily better adapted to the increasing temperatures and frequency of heatwaves. Newer building envelopes have better insulation, but in summertime, it shows to be detrimental in retaining too much heat. Another reason could be that the ceiling height and room sizes are much smaller in residential buildings, as compared to classrooms and hospital rooms.

And finally, a significant finding in optimizing the process of finding mitigation solutions for buildings is to build upon the solutions used in previous extreme years. With the hospital and residential building, each mitigation strategy was first applied to the building for each year and then combinations of mitigation techniques were used to find a solution for each year. For School 3, the building was assessed one year at a time, first finding a solution for 2020 and then using that solution as a starting point to find a solution for overheating in 2044. In this way, less simulations need to be run and it is easier to create a clear path in the installation of these devices, as is shown in the Table 45 that summarizes the suggested mitigation strategies to be installed by that year in addition to what has been installed in the previous year. And so, for example, School 3 will require the installation of exterior shade rolls immediately to mitigate short-term overheating, then add a cool roof to resolve mid-term overheating and finally install overhangs to resolve long-term overheating.

Given the findings from the overheating risk assessments which did not involve improvements to the building envelope, it is essential to consider that the existing buildings may require building envelope upgrades to meet energy requirements by 2044 and 2090. Upgrading the building envelope to code requirements is an essential step to enhance energy efficiency and optimize indoor thermal conditions and should be considered before evaluating the risk of overheating and application of mitigation strategies. These modifications can play a significant role in adapting the buildings to cope with increasing temperatures and the frequency of heatwaves, and their incorporation into the overall mitigation approach should be carefully evaluated.

Table 45: Summary of mitigation strategies to install by year

Building	**2020**	**2044**	**2090**
School 3	exterior shade rolls	cool roof	overhangs
School 4	exterior shade rolls	night cooling	cool roof
Hospital 1	exterior shade roll or sidefins	cool wall	exchange or add sidefins for exterior shade roll
Residential 1	exterior shade roll	--	cool roof and cool wall

7. Conclusion

7.1. Conclusion

This thesis applied two different building calibration methodologies to assess and mitigate overheating risks in six existing buildings. The MOGA calibration method was chosen, due to its higher precision and ease of use in the simultaneous calibration of individual rooms within one building. Using this method allowed the calibration of 4 schools, 1 hospital and 1 residence. The application of this calibration method was validated with each case and the assessment and mitigation of overheating risks in these buildings was performed, closing a knowledge gap in the calibration of building models for the risk assessment in summertime overheating in Canada. Several mitigation techniques were proven sufficient in adapting these buildings for current and future climate, such as exterior roll shades, night cooling, exterior shading (overhangs or sidefins) and cool walls and/or roofs.

7.2. Contributions

Major contributions of the work presented in this paper include the validation and repeatability of two novel calibration techniques: Bayesian calibration and multi-objective genetic algorithm. The first school was calibrated using both Bayesian calibration and multi-objective genetic algorithm, which produced highly precise results with margins of error significantly smaller than existing calibration methods and standards. The use of both methods on one school also showed the differences in results and the advantages and disadvantages of each method. Having decided that MOGA was more suited for the task at hand, this procedure was refined and repeated over 5 other buildings, including 3 schools, 1 hospital and 1 residential building, which all yielded acceptable results with high level of precision as calculated using the performance metrics. Throughout the calibration process on these buildings, both the calibration methodology and evaluation criteria performed well and have good repeatability over many buildings of the same type and of different types. Other contributions include: finding the building parameters which have the most impact on the indoor temperature of the buildings; the calibration process of modifying building inputs, as shown in Table 28; using future weather data instead of typical weather data to assess buildings for overheating; using mitigation strategies in building simulation to predict their impact on reducing overheating hours; and providing a timeline to apply multiple mitigation strategies in combination over time to mitigate overheating risks.

7.3. Future Work

These methods should be used to create user-friendly programs, where inputs can be minimized to maximize productivity and stability of the code. While some moderate to extensive background in building science, computer-aided modeling and reading program code is required to make use of both calibration methods explored in this study, it would be interesting to create a user interface in which a client with limited knowledge would be able to input a small dataset concerning a building's parameters and measured data to produce a calibrated model of their buildings. It would also be interesting to connect existing thermostats to a program to record indoor temperature as an added source of information to continuously calibrate a building model from measured data.

8. Bibliography

Adeyemo, A. & Amusan, O. (2022). Modelling and multi-objective optimization of hybrid energy storage solution for photovoltaic powered off-grid net zero energy building. *Journal of Energy Storage, 55.* https://doi.org/10.1016/j.est.2022.105273.

Alim, M., Rahman, A., Tao, Z., Garner, B., Griffith, R. & Liebman, M. (2022). Green roof as an effective tool for sustainable urban development: An Australian perspective in relation to stormwater and building energy management. *Journal of Cleaner Production, 362,* 132561. https://doi.org/10.1016/J.JCLEPRO.2022.132561.

Aparicio-Ruiz, P., Barbadilla-Martin, E., Guadix, J. & Munuzuri, J. (2021). A field study on adaptive thermal comfort in Spanish primary classrooms during summer season. *Building and Environment, 203,* 108089. https://doi.org/10.1016/J.BUILDENV.2021.108089.

Ascione, F., De Masi, R., Festa, Vl, Mauro, G. & Vanoli, G. (2023). Optimizing space cooling of a nearly zero energy building via model predictive control: Energy cost vs comfort. *Energy and Buildings, 278.* https://doi.org/10.1016/j.enbuild.2022.112664.

Ascione, F., De Massi, R., Mastellone, M., Ruggiero, S. & Vanoli, G. (2020). *Energies, 13(9).* https://doi.org/10.3390/en13092296.

Azevedo, L., Gomes, R. & Silva, C. (2021). Influence of model calibration and optimization techniques on the evaluation of thermal comfort and retrofit measures of a Lisbon household using building energy simulation. *Advances in Building Energy Research, 15(5),* 630-661. https://doi.org/10.1080/17512549.2019.1654916.

Azevedo, L., Gomes, R. & Silva, C. (2021). Influence of model calibration and optimization techniques on the valuation of thermal comfort and retrofit measures of a Lisbon household using building energy simulation. *Advances in Building Energy Research, 15(5),* 630-661. https://doi.org/10.1080/17512549.2019.1654916.

Baba, F. M. (2022). Assessment and Mitigation of Overheating Risks in Archetype and Existing Canadian Buildings under Recent and Projected Future Climates [Doctoral dissertation, Concordia University].

Baba, F., Ge, H., Wang, L. & Zmeureanu, R. (2022). Do high energy-efficient buildings increase overheating risk in cold climate? Causes and mitigation measures required under recent and future climates. *Building and Environment, 219,* 109230. https://doi.org/10.1016/J.BUILDENV.2022.109230.

Baba, F., Ge, H., Wang, L. & Zmeureanu, R. (2023). Assessing and mitigating overheating risk in existing Canadian school buildings under extreme current and future climates. *Energy and Buildings, 279,* 112710. https://doi.org/10.1016/J.ENBUILD.2022.112710.

Baba, F., Ge, H., Zmeureanu, R. & Wang, L. (2022). Calibration of building model based on indoor temperature for overheating assessment using generic algorithm: Methodology,

evaluation criteria, and case study. *Building and Environment, 207,* 108518. https://doi.org/10.1016/J.BUILDENV.2021.108518.

Baghoolizadeh, M., Nadooshan, A., Dehkordi, S., Rostamzadeh-Renani, M., Roztamzadeh-Renani, R. & Afrand, M. (2022). Multi-objective optimization of annual electricity consumption and annual electricity production of a residential building using photovoltaic shadings. *International Journal of Energy Research, 46(15),* 21172-21216. https://doi.org/10.1002/er.8401.

Bahdad, A., Fadzil, S., Onubi, H. & BenLasod, S. (2022). Multi-dimensions optimization for optimum modifications of light-shelves parameters for daylighting and energy efficiency. *International Journal of Environmental Science and Technology, 19(4),* 2659-2676. https://doi.org/10.1007/s13762-021-03328-9.

Berardi, U. & Jafarpur, P. (2020). Assessing the impact of climate change on building heating and cooling energy demand in Canada. *Renewable and Sustainable Energy Reviews, 121*, 109681. https://doi.org/10.1016/J.RSER.2019.109681.

Berardi, U. Garai, M. & Morselli, T. (2020). Preparation and assessment of the potential energy savings of thermochromic and cool coatings considering inter-building effects. *Solar Energy, 209,* 493-504. https://doi.org/10.1016/J.SOLENER.2020.09.015.

Booluk, S. & Seyis, S. (2022). Review of Uncertainties in Building Characterization for Urban-Scale Energy Modeling. *Communications in Computer and Information Science,* 159-182. https://doi.org/10.1007/978-3-031-16895-6_11.

Boyd, D., Pathak, M., van Diemen, R & Skea, J. (2022). Mitigation co-benefits of climate change adaptation: A case-study analysis of eight cities. *Sustainable Cities and Society, 77,* 103563. https://doi.org/10.1016/J.SCS.2021.103563.

Calama-Gonzalez, C., Suarez, R. & Leon Rodriguez, A. (2022). Thermal comfort prediction of the existing housing stock in southern Spain through calibrated and validated parameterized simulation models. *Energy and Buildings, 254.* https://doi.org/10.1016/j.enbuild.2021.111562.

Calama-Gonzalez, C., Symonds, P., Leon-Rodriguez, A. & Suarez, R. (2022). Optimal retrofit solutions considering thermal comfort and intervention costs for the Mediterranean social housing stock. *Energy and Buildings, 259.* https://doi.org/10.1016/j.enbuild.2022.111915.

Calama-Gonzalez, C., Symonds, P., Petrou, G., Suarez, R. & Leon-Rodriguez, A. (2021). Bayesian calibration of building energy models for uncertainty analysis through test cells monitoring. *Applied Energy, 282.* https://doi.org/10.1016/j.apenergy.2020.116118.

Chidiac, S., Yao, L. & Liu, P. (2022). Climate Change Effects on Heating and Cooling Demands of Buildings in Canada. *CivilEng, 3(2),* 277-295. https://doi.org/10.390/civileng3020017.

Chinazzo, G., Andersen, R., Azar, E., Barthelmes, V., Becchio, C., Belussi, L., Berger, C., Carlucci, S., Corgnati, S., Crosby, S., Danza, L., de Castro, L, Favero, M., Gautheir, S., Hellwig, R., Jin, Q., Kim, J., Sarey, Khanie, M., Khovalyg, D., Lingua, C., Luna-Navarro, A., Mahdavi, A., Miller, C., Mino-Rodriguez, I., Pigliautile, I., Pisello, A., Rupp, R., Saddick, A., Salamone, F., Scheweiker, M., Syndicus, M., Sigliantini, G., Vasquez, N., Vakalis, D., Vellei, M. & Wei, S. (2022). Quality criteria for multi-domain studies in the indoor environment: Critical review towards research guidelines and recommendations. *Building and Environment, 226,* 109719. https://doi.org/10.1016/J.BUILDENV.2022.109719.

Chinde, V., Lin, Y. & Ellis, M. (2022). Data-Enabled Predictive Control for Building HVAC Systems. *Journal of Dynamic Systems, Measurement, and Control, 144(8).* https://doi.org/10.1115/1.4054314.

Cho, J. & Moon, J. (2022). Integrated artificial neural network prediction model of indoor environmental quality in a school building. *Journal of Cleaner Production, 344.* https://doi.org/10.1016/j.jclepro.2022.131083.

Chong, A., Augenbroe, G. & Yan, D. (2021). Occupancy data at different spatial resolutions: Building energy performance and model calibration. *Applied Energy, 286.* https://doi.org/10.1016/j.apenergy.2021.116492.

Ciulla, G. & D'Amico, A. (2019). Building energy performance forecasting: A multiple linear regression approach. *Applied Energy, 253,* 113500. https://doi.org/10.1016/J.APENERGY.2019.113500.

Defo, M. & Lacasse, M. (2022). Resilience of Canadian residential brick veneer wall construction to climate change. *IOP Conference Series: Earth and Environmental Science.* https://doi.org/10.1088/1755-1315/1101/2/022019.

Defo, M. & Lacasse, M. (2022). Resilience of Canadian residential brick veneer wall construction to climate change. *IOP Conference Series: Earth and Environmental Science.* https://doi.org/10.1088/1755-1315/1101/2/022019.

Demis Dilsiz, A., Ng, K., Kampf, J. & Nagy, Z. (2022). Ranking parameters in urban energy models for various building forms and climates using sensitivity analysis. *Building Simulation.* https://doi.org/10.1007/s12273-022-0961-5.

Derakhti, M., O'Brien, W. & Bucking, S. (2022). Impact of measured data frequency on commercial building energy model calibration for retrofit analysis. *Science and Technology for the Built Environment, 28(5),* 628-644. https://doi.org/10.1080/23744731.2021.1991177.

Escandon, R., Suarez, R., Alonso, A. &Maura, G. (2022). Is indoor overheating an upcoming risk in southern Spain social housing stocks? Predictive assessment under a climate change

scenario. *Building and Environment, 207,* 108482. https://doi.org/10.1016/J.BUILDENV.2021.108482.

Faraji, A., Rashidi, M., Rezaei, F. & Rahnamayiezekavat, P. (2023). A Meta-Synthesis Review of Occupant Comfort Assessment in Buildings (2002-2022). *Sustainability (Switzerland), 15(5).* https://doi.org/10.3390/su15054303.

Fu, Y., Li, X., Zhou, X., Geng, X., Guo, Y. & Zhang, Y. (2020). Progress in plant phenology modeling under global climate change. *Science China Earth Sciences, 63(9),* 1237-1247. https://doi.org/10.1007/s11430-019-9622-2.

Gan, V., Luo, H., Tan, Y., Deng, M. & Kwok, H. (2021). Bim and data-driven predictive analysis of optimum termal comfort for indoor environment. *Sensors, 21(13).* https://doi.org/10.3390/s21134401.

Gao, B., Zhu, X., Ren, J., Ran, J., Kim, M. & Miu, J. (2023). Multi-objective optimization of energy-saving measures and operation parameters for a newly retrofitted building in future climate conditions: A case study of an office building in Chengdu. *Energy Reports, 9,* 2269-2285. https://doi.org/10.1016/J.EGYR.2023.01.049.

Gatt, D., Yousif, C., Cellura, M., Camilleri, L. & Guarino, F. (2020). Assessment of building energy modelling studies to meet the requirements of the new Energy Performance of Buildings Directive. *Renewable and Sustainable Energy Reviews, 127.* https://doi.org/10.1016/j.rser.2020.109886.

Gilani, S. & O'Brien, W. (2021). Natural ventilation usability under climate change in Canada and the United States. *Building Research and Information, 49(4).* 376-386. https://doi.org/10.1080/09613218.2020.1760775.

Gilani, S. & O'Brien, W. (2021). Natural ventilation usability under climate change in Canada and the United States. *Building Research & Information, 49(4),* 367-386. https://doi.org/10.1080/09613218.2020.1760775.

GISS Surface Temperature Analisis (GISTEMP), version 4 (2023). *NASA Goddard Institute for Space Studies*. https://data.giss.nasa.gov/gistemp/

Gouvernement du Quebec. (2017). *Québec Public Infrastructure Plan 2017-2027 Report - Appendix 2: detailed inventory school boards*. Montreal, QC: Bibliotheque et Archives nationales du Quebec.

Gupta, S., Chanda, P. & Biswas, A. (2023). A 2E, energy and environment performance of an optimized vernacular house for passive cooling – Case of North-East India. *Building and Environment, 229.* https://doi.org/10.1016/j.buildenv.2022.109909.

He, Z., Gao, M., Li, Z., Guo, Z., Ke, S., Qi, Z., Tu, X., Du, B., Lai, X. (2023). Parametrized multi-objective seismic optimization for precast concrete frame with a novel post-

tensioned energy dissipation beam-column joint. *Computers and Structures, 275.* https://doi.org/10.1016/j.compstruc.2022.106911.

Hengl, T., Nussbaum, M., Wright, M., Heuvelink, G. & Graeler, B. (2018). Random forest as a generic framework for predictive modeling of spatial and spatio-temporal variables. *PeerJ.* https://doi.org/10.7717/peerj.5518.

Hosamo, H., Tingstveit, M., Nielsen, H., Svennevig, P. & Svidt, K. (2022). Multiobjective optimization of building energy consumption and thermal comfort based on integrated BIM framework with machine learning – NSGA II. *Energy and Buildings, 277.* https://doi.org/10.1016/j.enbuild.2022.112479.

Hou, D., Hassan I. & Wang, L. (2021). Bayesian Inference Calibration of Building Energy Models for Arid Weather. *ASME 2021 Verification and Validation Symposium.* https://doi.org/10.1115/vvs2021-65256.

Hou, D., Hassan, I. & Wang, L. (2021). Review on building energy model calibration by Bayesian inference. *Renewable and Sustainable Energy Reviews, 143.* https://doi.org/10.1016/j.rser.2021.110930.

Hou, D., Shu, C., Ji, L., Hassan, I. & Wang, L. (2021). Bayesian calibrating educational building thermal models to hourly indoor air temperature: Methodology and case study. *Proceedings of the 2021 ASME Verification and Validation Symposium.* https://doi.org/10.1115/VVS2021-65268.

Ide, L., Gutland, M., Bucking, S. &Santana Quintero, M. (2022). Balancing Trade-offs between Deep Energy Retrofits and Heritage Conservation: A Methodology and Case Study. *International Journval of Architectural Heritage, 16(1).* 97-116. https://doi.org/15583058.2020.1753261.

Jeong, K., Hong, T., Kim, J. & Cho, K. (2019). Development of a multi-objective optimization model for determining the optimal CO2 emissions reduction strategies for a multi-family housing complex. *Renewable and Sustainable Energy Reviews, 110,* 118-131. https://doi.org/10.1016/j.rser.2019.04.068.

Ji, L., Laouadi, A., Shu, C., Gaur, A., Lacasse, M. & Wang, L. (2022). Evaluating approaches of selecting extreme hot years for assessing building overheating conditions during heatwaves. *Energy and Buildings, 254,* 111610. https://doi.org/10.1016/J.ENBUILD.2021.111610.

Ji, Y., Swan, W., Fitton, R. & Fernando, T. (2019). Assessing the requirements from 'BB101' 2006 and 2018 for a naturally ventilated preparatory school in the UK. *Building Services Engineering Research and Technology, 40(5),* 638-359. https://doi.org/10.1177/0143624418815785.

Katal, A., Leroyer, S., Zou, J., Nikiema, O., Albettar, M., Belair, S. & Wang, L. (2023). Outdoor heat stress assessment using an integrated multi-scale numerical weather prediction system: A case study of a heatwave in Montreal. *Science of The Total Environment, 865,* 161276. https://doi.org/10.1016/J.SCITOTENV.2022.161276.

Khovalyg, D., Kazanci, O., Halvorsen, H., Gundlach, I., Bahnfleth, W., Toftum, J. & Olesen, B. (2020). Critical review of standards for indoor thermal environment and air quality. *Energy and Buildings, 213,* 109819. httpsL//doi.org/10.1016/J.ENBUILD.2020.109819.

Kim, H., Bilionis, I., Karava, P. & Braun, J. (2023). Human decision making during eco-feedback in smart and connected energy-aware communities. *Energy and Buildings, 278.* https://doi.org/10.1016/j.enbuild.2022.112627.

Kim, J., Kim, E., Kapsis, K. & Lacroix, D. (2023). An integrated Framework for the Design of Climate-Resilient Buildings in Canada. *Proceedings of the Canadian Society of Civil Engineering Annual Conference 2021,* 597-608.

Kumar, D., Alam, M. & Sanjayan, J. (2022). Building Datpation to Extreme Heatwaves. *Springer Tracts in Civil Engineering,* 189-216. https://doi.org/10.1007-978-3-030-85018-0_9.

Kumar, D., Alam, M., Memon, R. & Bhayo, B. (2022). A critical review for formulation and conceptualization of an ideal building envelope and novel sustainability framework for building applications. *Cleaner Engineering and Technology, 11,* 100555. https://doi.org/10.1016/J.CLET.2022.100555.

Laouadi, A., Ji, L., Shu, C., Wang, L. & Lacasse, M. (2023). Overheating Risk Analysis in Long-Term Care Homes – Development of Overheating Limit Criteria. *Buildings, 13(2).* https://doi.org/10.3390/nuildings13020390.

Lenssen, N., Schmidt, G., Hanswen, J., Menne, M., Persin, A., Ruedy, R. & Zyss, D. (2019). Improvements in the GISTEMP Uncertainty Model. *Journal of Geophysical Research: Atmospheres, 124 (12),* 6307-6326. https://doi.org/10.1029/2018JD029522.

Li, J., Zhao, T., Wang, P., Yoon, S. & Yu, Y. (2020). Effects of various partitions on the accuracy of virtual in-situ calibration in building energy systems. *Journal of Building Engineering, 32,* 101538. https://doi.org/10.1016/J.JOBE.2020.101538.

Li, W., Tian, Z., Lu, Y. & Fu, F. (2018). Stepwise calibration for residential building thermal performance model using hourly heat consumption data. *Energy and Buildings, 181,* 10-25. https://doi.org/10.1016/J.ENBUILD.2018.10.001.

Lim, H. & Zhai, Z. (2018). Influences of energy data on Bayesian calibration of building energy model. *Applied Energy, 231,* 686-698. https://doi.org/10.1016/J.APENERGY.2018.09.156.

Lim, H. & Zhai, Z. (2020). Prediction of Building Stock Energy Demand. *Environmental Science and Engineering,* 1305-1314. https://doi.org/10.1007/978-981-13-9528-4_132.

Lim, H. & Zhai, Z. (2022). Estimating unknown parameters of a building stock using a stochastic-deterministic-coupled approach. *Energy and Buildings, 255.* https://doi.org/10.1016/j.enbuild.2021.111673.

Mahmoud, S. Saad, M., Elshelfa, M., Abdelkhalik, H. & Fahmy, M. (2022). Comparative Analysis of Occupant Thermal Comfort, Energy Consumption, and CO2 Emissions for an Educational Building in Cold Climate: A Case Study in Canada. *IOP Conference Series: Earth and Environmental Science*, *1056(1),* 012027. https://doi.org/10.1088/1755-1315/1056/1/012027.

Martinez, S, Eguia, P., Granada, E., Moazami, A. & Hamdy, M. (2020). A performance comparison of multi-objective optimization-based approaches for calibrating white-box building energy models. *Energy and Buildings, 216.* https://doi.org/10.1016/j.enbuild.2020.109942.

Martinez, S., Eguia, P., Granada, E., Moazami, A. & Hamdy, M. (2020) A performance comparison of multi-objective optimization-based apparoaches for calibrating white-box building energy models. *Energy and Buildings, 216.* https://doi.org/10.1016/j.enbuild.2020.109942.

Martinez, S., Perez, E., Eguia, P., Erkoreka, A. & Granada, E. (2020). Model calibration and exergoeconomic optimization with NSGA-II Applied to a residential cogeneration. *Applied Thermal Engineering, 169*. https://doi.org/10.1016/j.applthermaleng.2020.114916.

Moradi, A., Kavgic, M., Costanzo, V. & Evola, G. (2023). Impact of typical and actual weather years on the energy simulation of buildings with different construction features and under different climates. *Energy, 270,* 126875. https://doi.org/10.1016/J.ENERGY.2023.126875.

Morey, J., Beizaee, A. & Wright, A. (2020). An investigation into overheating in social housing dwellings in central England. *Building and Environment, 176,* 106814. https://doi.org/10.1016/J.BUILDENV.2020.106814.

Oetomo, A., Jalali, N., Costa, P. & Morita, P. (2022). Indoor Temperatures in the 2018 Heat Wae in Quebec, Canada: Exploratory Study Using Ecobee Smart Thermostats. *JMIR Form Res, (5).* https://doi.org/10.2196/34104.

Oliver, A., Leoto, R., Lizzaralde, G., Petter, A. & Roy, N. (2019). Design, decision-making and trade-offs in the Centre for Sustainable Development (La Maison du developpement durable) in Canada. *IOP Conference Series:Earth and Environmental Science, 294(1),* 012055. https://doi.org/10.1088/1755-1315/294/1/012055.

Oregi, X., Hermoso, N., Arrizabalaga, E., Mabe, L. & Munoz, I. (2018). Sensitivity assessment of a district energy assessment characterisation model based on cadastral data. *Energy Procedia, 147,* 181-188. https://doi.org/10.1016/J.EGYPRO.2018.07.053.

Oxariosoy, B. (2022). Energy effectiveness of passive cooling design strategies to reduce the impact of long-term heatwaves on occupants' thermal comfort in Europe: Climate change and mitigation. *Journal of Cleaner Production, 330,* 129675. https://doi.org/10.1016/J.JCLEPRO.2021.129675

Panica, S., Larcher, M., Marincioni, V., Troi, A., Baglivo, C. & Congedo, P. (2023). Identifying key parameters through a sensitivity analysis for realistic hygrothermal simulations at wall level supported by monitored data. *Building and Environment, 229*, 109969. https://doi.org/10.1016/J.BUILDENV.2022.109969.

Prabatha, T., Hewage, K., Karunathilake, H. & Sadiq, R. (2020). To retrofit or not? Making energy retrofit decisions through life cycle thinking for Canadian residences. *Energy and Buildings, 226,* 110393. https://doi.org/10.1016/J.ENBUILD.2020.110393.

Prataviera, E., Vivian, J., Lombardo, G. & Zarrella, A. (2022). Evaluation of the impact of input uncertainty on urban building energy simulations using uncertainty and sensitivity analysis. *Applied Energy, 311,* 118691. https://doi.org/10.1016/J.APENERGY.2022.118691.

Qiu, S., Li, Z., Pang, Z., Zhang, W. & Li, Z. (2018). A quick auto-calibration approach based on normative energy models. *Energy and Buildings, 172,* 35-46. https://doi.org/10.1016/j.enbuild.2018.04.053.

Qiu, S., Li, Z., Pang, Z., Zhang, W. & Li, Z. (2018). A quick auto-calibration approach based on normative energy models. *Energy and Buildings, 172,* 35-42. https://doi.org/10.1016/J.ENBUILD.2018.04.053.

Rahif, R., Hamdy, M., Homaei, S., Zhang, C., Holzer, P. & Attia, S. (2022). Simulation-based framework to evaluate resistivity of cooling strategies in buildings against overheating impact of climate change. *Building and Environment, 208,* 108599. https://doi.org/10.1016/J.BUILDENV.2021.108599.

Rana, A., Perera, P., Ruparathna, R., Karunathilake, H., Hewage, K., Alam, M. & Sadiq, R. (2020) Occupant-based energy upgrades selection for Candian residential buildings based on field energy data dna calibrated simulations. *Journal of Cleaner Production, 271*, 122430. https://doi.org/10.1016/J.JCLEPRO.2020.122430.

Risch, S. Remmen, P. &Muller, D. (2021). Influence of data acquisition on the Bayesian calibration of urban building energy models. *Energy and Buildings, 230.* https://doi.org/10.1016/j.enbuild.2020.110512.

Roumi, S., Zhang, F., Stewart, R. & Santamouris, M. (2023). Weighting of indoor environment quality parameters for occupant satisfaction and energy efficiency. *Building and Environment, 228,* 109898. https://doi.org/10.1016/J.BUILDENV.2022/109898.

Ruggiero, S., Iannantuono, M., Fortopoulou, A., Papadaki, D., Assimakopoulos, M., De Massi, R., Vanoli, G. & Ferrante, A. (2022). Multi-Objective Optimixation for Cooling and Interior Natural Lighitng in Buildings for Sustainable Renovation. *Sustainability (Switzerland), 14(13).* https://doi.org/10.3390/su14138001.

Saryazdi, S., Etemad, A., Shafaat, A. & Bahman, A. (2022). Data-driven performance analysis of a residential building applying artificial neural network (ANN) and multi-objective genetic algorithm (GA). *Building and Environment, 225.* https://doi.org/10.1016/j.buildenv.2022.109633.

Seghier, T., Lim, Y., Harun, M., Ahmad, M., Samah, A. & Majid, H. (2022). BIM-based retrofit method (RBIM) for building envelope thermal performance optimization. *Energy and Buildings, 256.* https://doi.org/10.1016.j.enbuild.2021.111693.

Shen, Y. & Yarnold, M. (2021). A novel sensitivity analysis of commercial building hybrid energy structure performance. *Journal of Building Engineering, 43,* 102808. https://doi.org/10.1016/J.JOBE.2021.102808.

Skillington, K., Crawford, R., Warren-Myers, G. & Davidson, K. (2022) A review of existing policy for reducing embodied energy and greenhouse gas emissions of buildings. *Energy Policy, 168,* 112920. https://doi.org/10.1016/J.ENPOL.2022.112920.

Soudian, S. & Berardi, U. (2022). Experimental performance evaluation of a climate-responsive ventilated building façade. *Journal of Building Engineering, 61,* 105233. https://doi.org/10.1016/J.JOBE.2022.105233.

Tardioli, G, Narayan, A., Kerrigan, R., Oates, M., O'Donnell, J. & Finn, D. (2020). A methodology for calibration of building energy models at distrct scale using clustering and surrogate techniques. *Energy and Buildings, 226.* https://doi.org/10.1016/j.enbuild.2020.110309.

Tariq, R., Torres-Aguilar, C., Zaman, J. Zavala-Guillen, I. Bassam, A., Ricalde, L. & Carvente, O. (2022). Digital twin models for optimization and global projection of building-integrated solar chimney. *Building and Environment, 213.* https://doi.org/10.1016/j.buildenv.2022.108807.

Vallianos, C., Athienitis, A. & Delcroix, B. (2022). Automatic generation of multi-zone RC models using smart thermostat data from homes. *Energy and Buildings, 277,* 112571. https://doi.org/10.1016/J.ENBUILD.2022112571.

Van Dronkelaar, C., Dowson, M., Spataru, C., Burman, E. & Mumovic, D. (2019). Quantifying the Underlying Causes of a Discrepancy Between Predicted and Measured Use. *Frontiers in mechanical Engineering, 5.* https://doi.org/10.3389/fmech.2019.00020.

Ville de Montréal. (2017). Climate Change Adaptation Plan for the Montreal Urban Agglomeration 2015-2020. 245 pages.

Wang, C., Tindemans, S., Miller, C., Agugiaro, G. & Stoter, J. (2020). Bayesian calibration at the urban scale: a case study on a large residential heating demand applicaiton in Amsterdam. *Journal of Building Performance Simulation, 13(3),* 347-361. https://doi.org/10.1080/19401493.2020.1729862.

Wang, R., Li, J., Ma, J. & Peng, W. (2022). The Characteristics of Thermal Environment and Comfort of Residential Buildings during Winter in Hot Summer and Cold Winter Climate Zone of China. *E3S Web of Conferences.* https://doi.org/10.1051/e3sconf/202235603027.

Wang, R., Lu, S., Feng, W. & Xu, B. (2021). Tradeoff betwen heating energy demand in winter and indoor overheating risk in summer constrained by building standards. *Building Simulation, 14(4),* 987-1003. https://doi.org/10.1007/s12273-020-0719-x.

Wang, Y., Yang, W. & Wang Q. (2022). Multi-objective parametric optimization of the composite external shading for the classroom based on lighting, energy consumption, and visual comfort. *Energy and Buildings, 275.* https://doi.org/10.1016/j.enbuild.2022.112441.

Westermann, P. Welzel, M. & Elvins, R. (2020). Using a deep temporal convolutional network as a building energy surrogate model that spans multiple climate zones. *Applied Energy, 278.* https://doi.org/10.1016/j.apenergy.2020.115563.

Wollschlaeger, S., Sadhu, A., Ebrahimi, G. & Woo, A. (2022). Investigation of climate change impacts on long-term care facility occupants. *City and Environment Interactions, 13*, 100077. https://doi.org/10.1016/J.CACINT.2021.100077.

Xia, W., Vuga, A., Jagota, V & Bhola, J. (2023) A Genetic Algorithm of Computer-Aided Architectural Design Based on BIM. *Computer-Aided Design and Applications, 20(S3),* 225-237. https://doi.org/10.14733/cadaps.2023.S3.225-237.

Xie, Z., Shu, C., Reich, B., Wang, L., Baril, D., Ji, L., Yang, S., Bai, X., Zmeureanu, R., Lacasse, M., Wang, L. & Ge, H. (2021). *Journal of Physics: Conference Series, 2069(1),* 012168. https://doi.org/10.1088/1742-6596/2069/1/012168.

Xie, Z., Shu, C., Reich, B., Wang, L., Baril, D., Ji, L., Yang, S., Bai, X., Zmeureanu, R., Lacasse, M., Wang, L. & Ge, H. (2021). A field study on summertime overheating of six schools in Montreal Canada. *Journal of Physics: Conference Series, 2069(1),* 012168. https://doi.org/10.188/1742-6596/2069/1/012168.

Yao, R., Zhang, S., Du, C., Scheweiker, M., Hodder, S., Olesen, B., Toftum, J., Romanada d<Ambrosio, F., Gebhardt, H., Zhou, S., Yuan, F. & Li, B. (2022). Evolution and performance analysis of adaptive thermal comfort models – A comprehensive literature review. *Building and Environment, 217,* 109020. https://doi.org/10.1016/J.BUILDENV.2022.109020.

Yuan, F., Yao, R., Sadrizadeh, S., Li, B., Cao, G., Zhang, S., Zhou, S., Liu, H., Bogdan, A., Croitoru, C., Melikove, Al, Short, C. & Li, B. (2022). Thermal comfort in hospital buildings – A literature review. *Journal of Building Engineering, 45,* 103463. https://doi.org/10.1016/J.JOBE.2021.103463.

Yuan, X., Heikari, L., Hirvonen, J., Liang, Y., Virtanen, M., Kosonen, R. & Pan, Y. (2022). System modelling and optimization of a low temeprature local hybrid energy system based on solar energy for a residential district. *Energy Conversion and Management, 267.* https://doi.org/10.1016/j.enconman.2022.115918.

Zhan, S., Wichern, G., Laughman, C., Chong, A. & Chakrabarty, A. (2022). Calibrating building simulation models using multi-source datasets and meta-learned Byesian optimization. *Energy and Buildings, 270.* https://doi.org/10.1016/j.enbuild.2022.112278.

Zhang, H., Feng, H, Hewage, K., Arashpour, M. (2022). Artificial Neural Network for Predicting Building Energy Performance: A Surrogate Energy Retrofits Decision Support Framework. *Buildings, 12(6).* https://doi.org/10.3390/buildings12060829.

Zhang, Z., Chong, A., Pan, Y., Zhang, C. & Lam, K. (2019). Whole building Energy model for HVAC optimal control: A practical framework based on deep reinforcement learning. *Energy and Buildings, 199,* 472-490. https://doi.org/10.1016/j.enbuild.2019.07.029.

Zhang, Z., Chong, Al, Pan, Y., Zhang, C. & Lam, K. (2019). Whole building energy model for HVAC optimal control: A practical framework based on deep reinforcement learning. *Energy and Buildings, 199,* 471-490. https://doi.org/10.1016/j.enbuild.2019.07.029.

Zhao, L., Zhang, W. & Wang, W. (2022). BIM-Based Multi-Objective Optimization of Low Carbon and Energy-Saving Buildings. *Sustainability (Switzerland), 14(20).* https://doi.org/10.3390/su142013064.

Zhong, L., Yuan, J. & Fleck, B. (2019). Indoor environmental quality evaluation of lecture classrooms in an institutional building in a cold climate. *Sustainability (Switzerland), 11(23).* https://doi.org/10.3390/su11236591.

Zhu, C., Tian, W., Yin, B., Li, Z. & Shi, J. (2020). Uncertainty calibration of building energy models by combining approximate Bayesian computation and machine learning algorithms. *Applied Energy, 268,* 115025. https://doi.org/10.1016/J.APENERGY.2020.115025.

9. Appendices

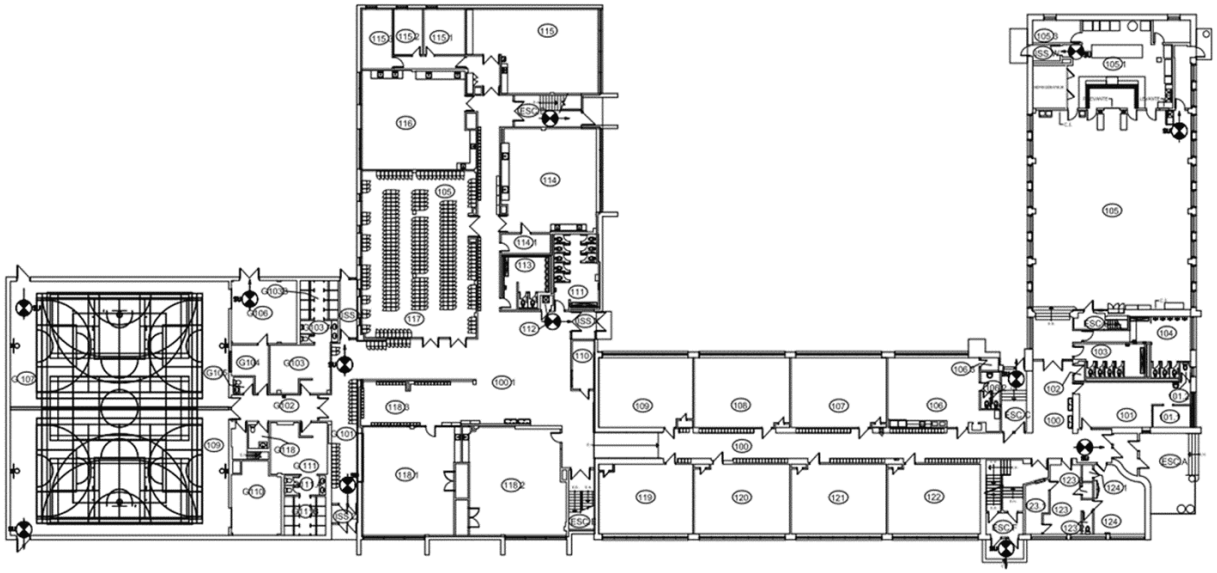

Figure 22: Floorplan of first floor of School 2

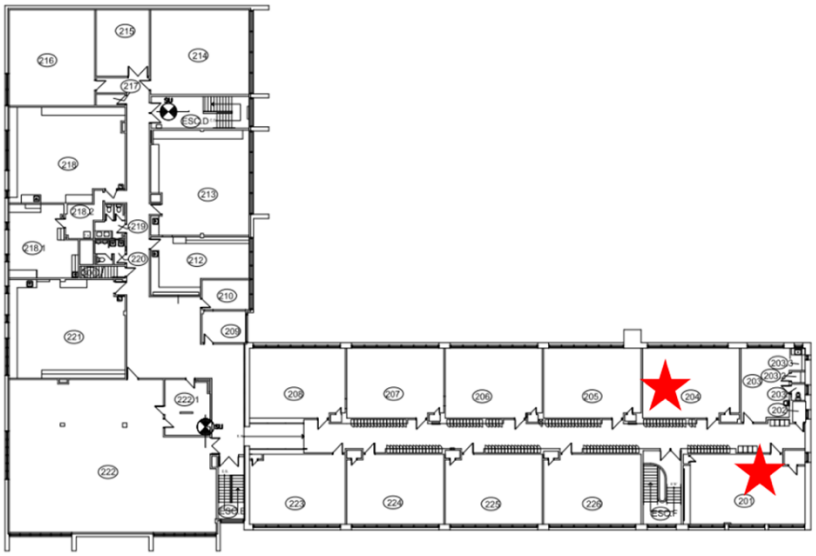

Figure 23: Floorplan of second floor of School 2

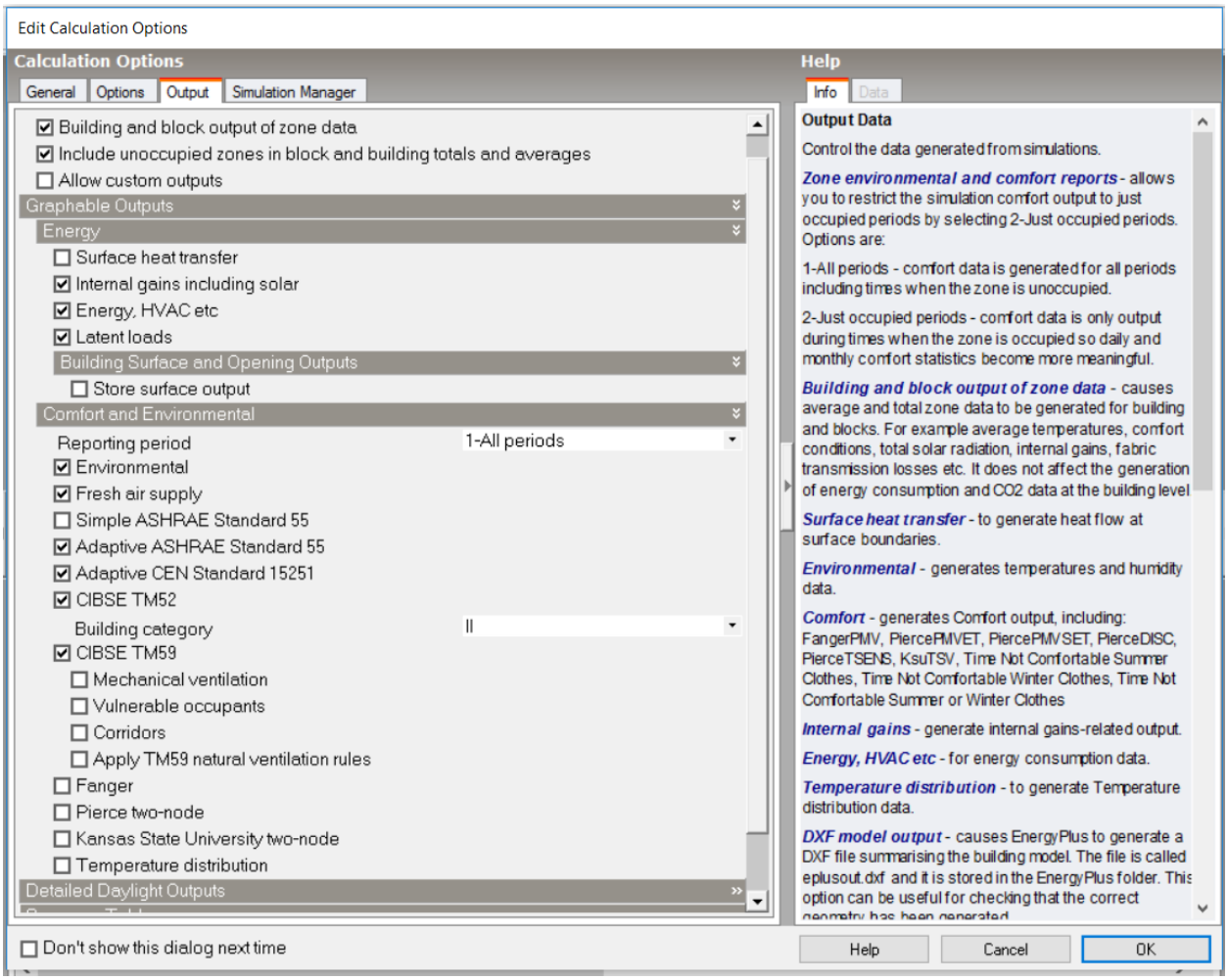

Figure 24: Simulation Options for Residential 1 in DesignBuilder

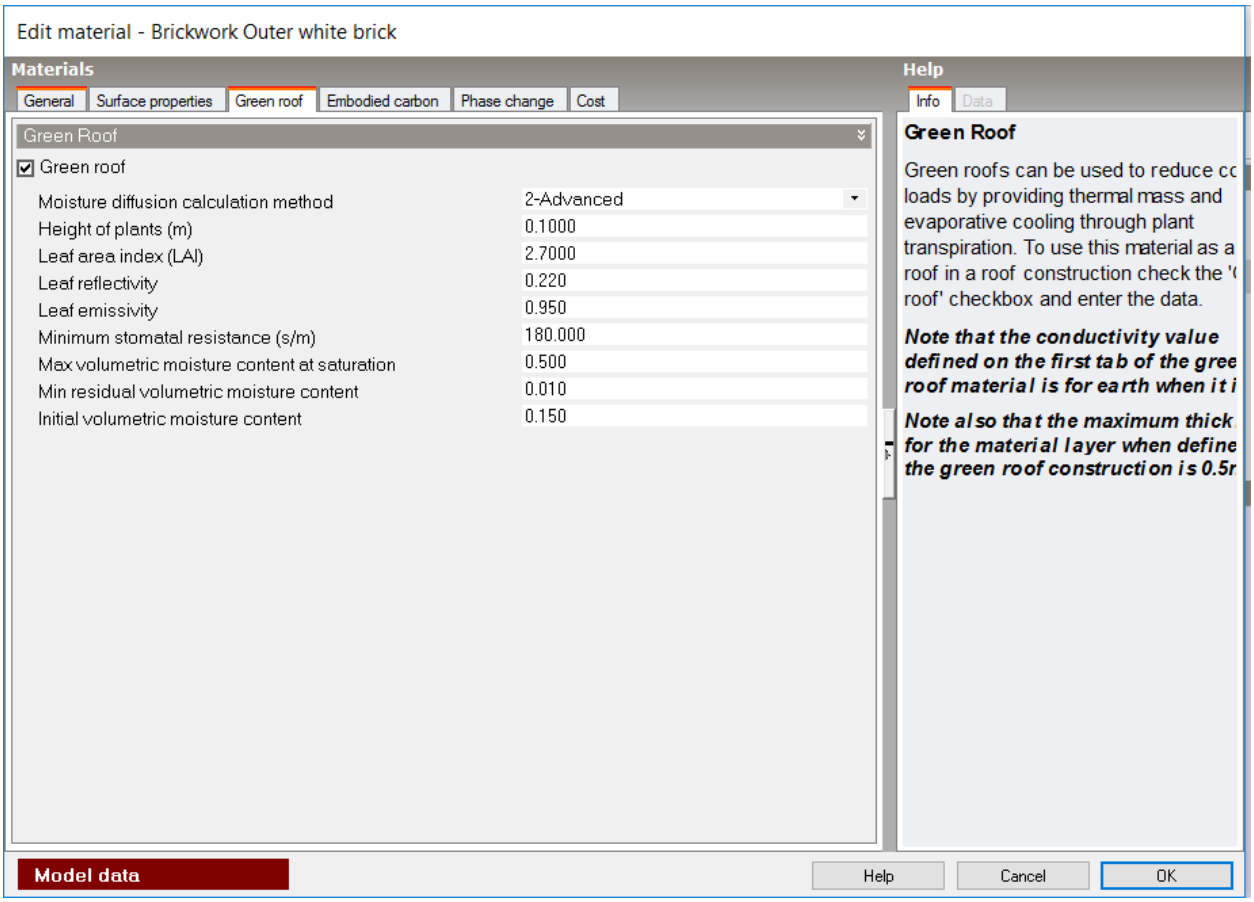

Figure 25: Snapshot of DesignBuilder for Green Roof Properties used for Hospital 1

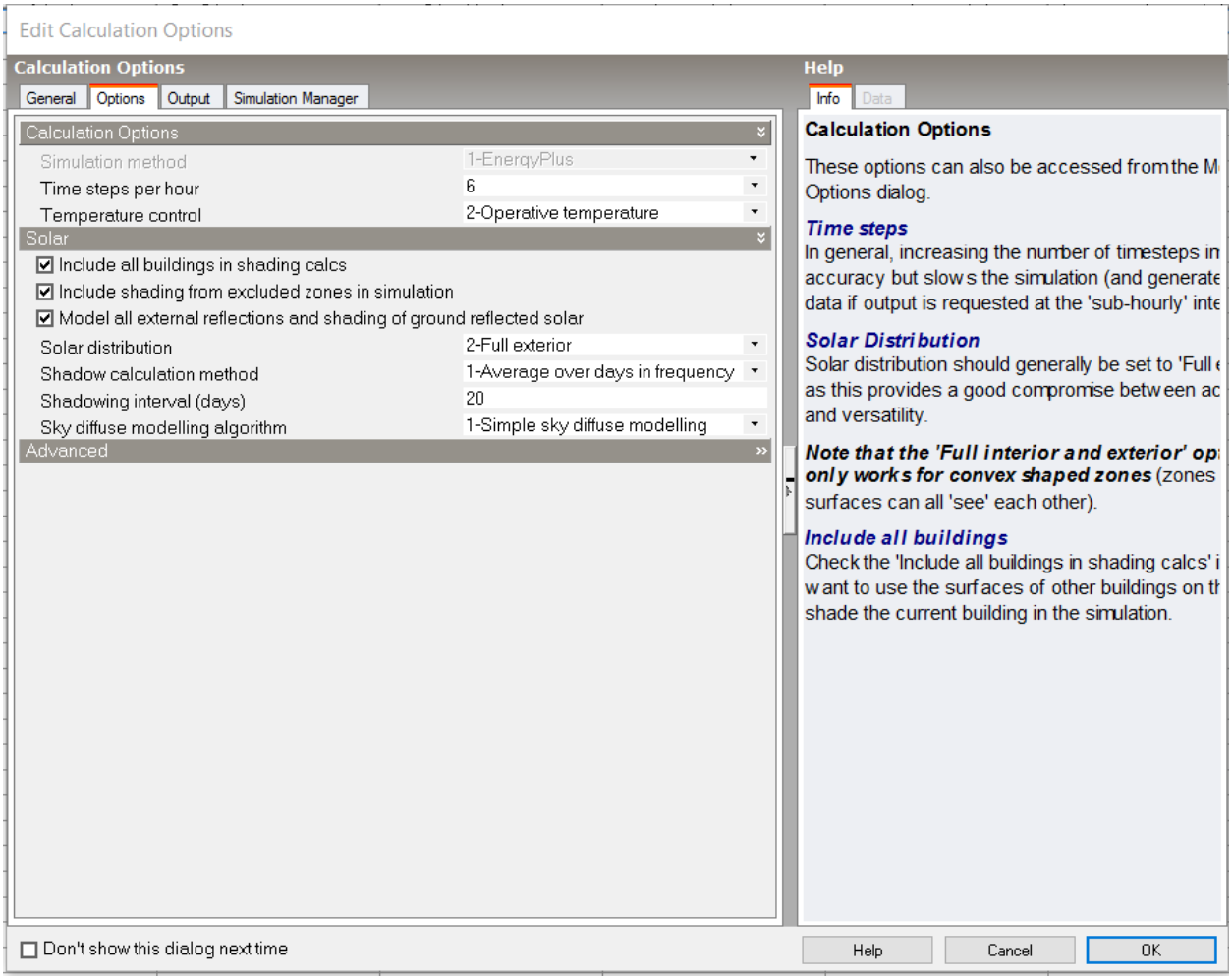

Figure 26: Snapshot from DesignBuilder of Simulation Options from School 3

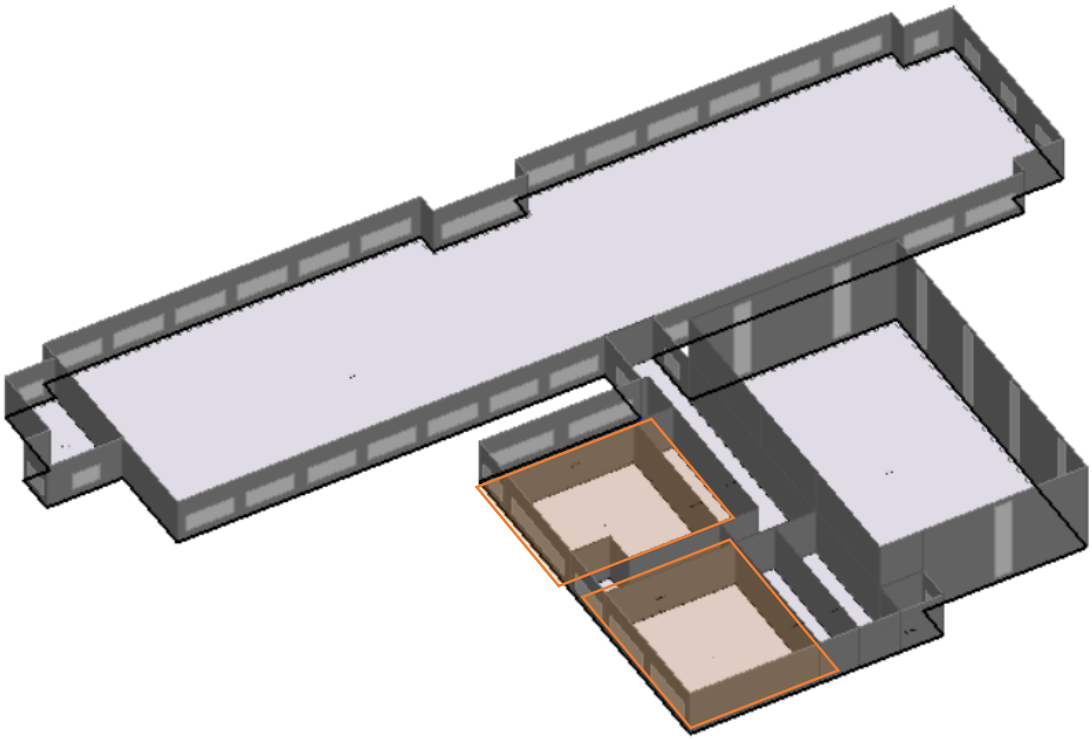

Figure 27: Axonometric view of first floor of School 4 in DesignBuilder

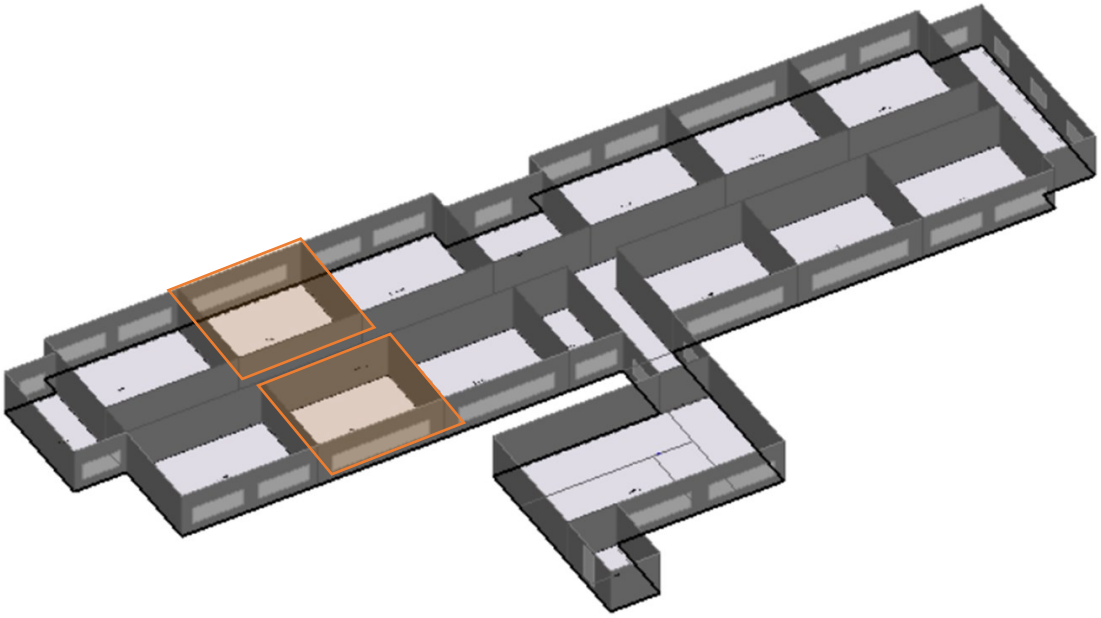

Figure 28: Axonometric view of second floor of School 4 in DesignBuilder

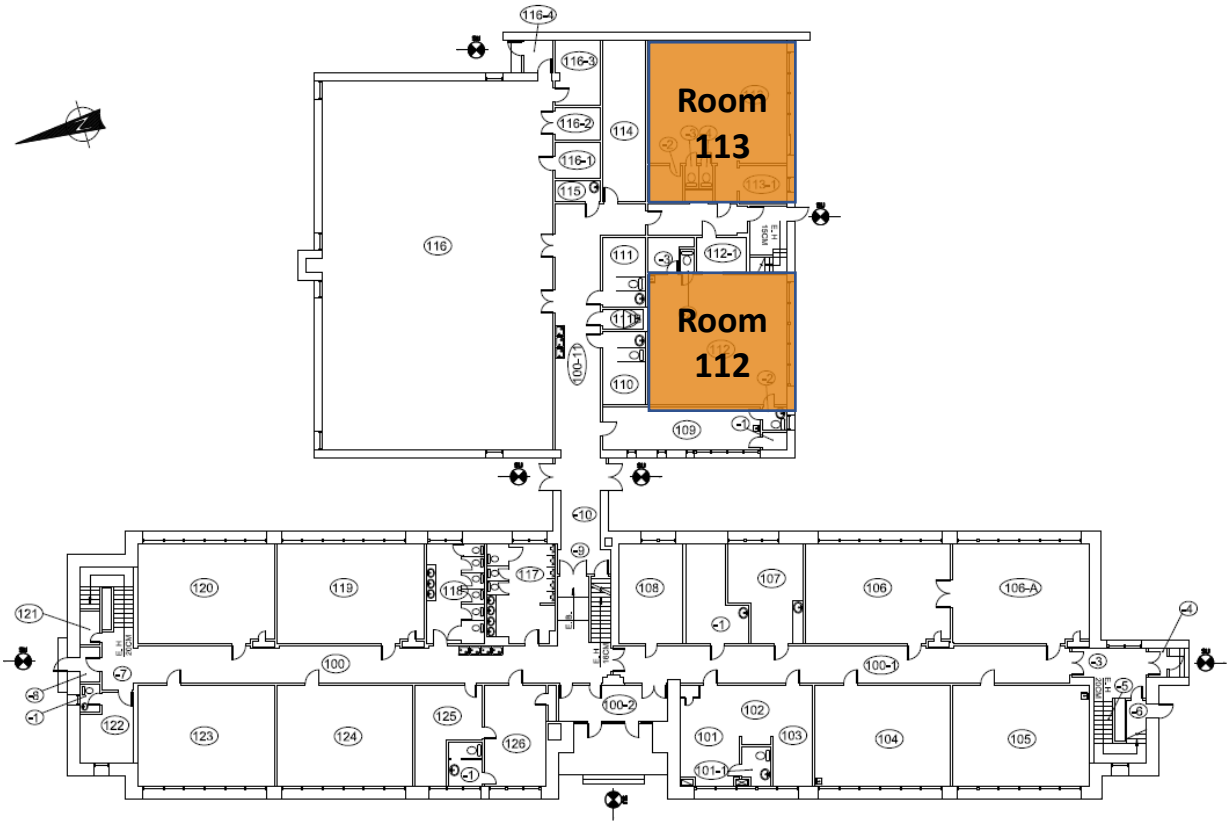

Figure 29: Plan view of first floor of School 4

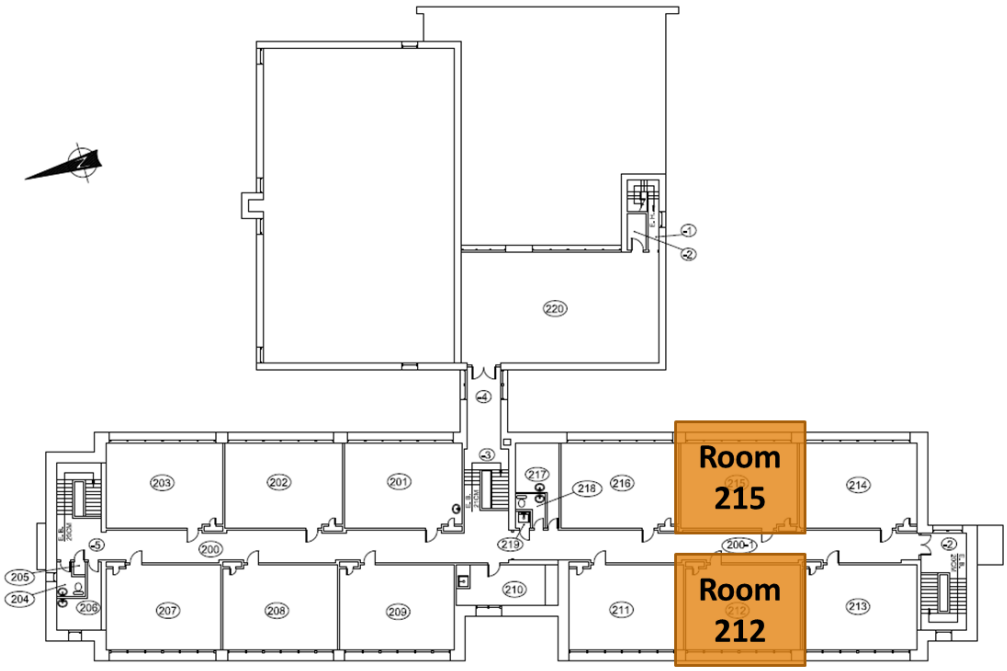

Figure 30: Plan view of second floor of School 4

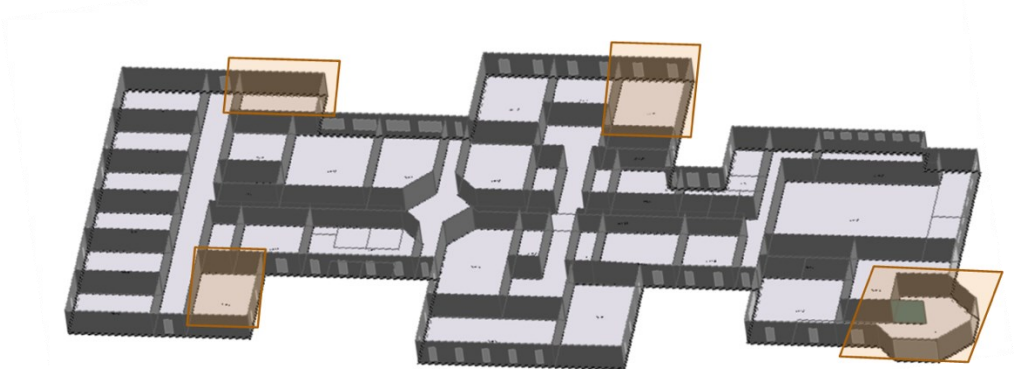

Figure 31: Axonometric Views of School 3 in DesignBuilder

Figure 32: Plan view of School 3 with the measured rooms identified

Figure 33: Photos of Room 112 from School 4

Figure 34: Room 212 before (left) and after (right) ceiling construction from School 4